Journal of Applied Polymer Science

Evaluation of Olefinic Block Copolymer Blends with Amorphous Polyolefins—Effect of Different Unsaturated and Saturated Hydrocarbon Tackifier Resins on Blend Miscibility

P. Rajesh Raja,[1] J. K. Wilson,[1] M. A. Peters,[1] S. G. Croll[2]

[1]Eastman Chemical Company, 100 N Eastman Road, Kingsport, Tennessee, 37662

[2]Department of Coatings and Polymeric Materials, North Dakota State University, Fargo, North Dakota , 58108

Correspondence to: P. Rajesh Raja (E-mail: rajeshp@eastman.com)

ABSTRACT: Blends of ethylene–octene based olefinic block copolymer (OBC) with two amorphous polyolefin (APO) polymers [atactic propylene homopolymer (PP) and ethylene–propylene copolymer (PE–PP)] were evaluated at three different ratios. Dynamic mechanical analysis (DMA) and transmission electron microscopy (TEM) evaluations were performed to determine the blend miscibility characteristics. Viscoelastic properties of both OBC blends with PP polymer, and OBC blends with PE–PP copolymer showed incompatibility. Analysis revealed that both blends formed two phase morphologies. The effect of three unsaturated aliphatic hydrocarbon resins with varying aromatic content and two saturated hydrocarbon resins with different chemistries were evaluated as compatibilizing agent for OBC/PP and OBC/PE–PP blends. A 1 : 1 polymer blend ratio of OBC/PP and OBC/PE–PP was selected to better understand the influence of resin addition at three different levels 20, 30, and 40 wt %. The fully aliphatic unsaturated resin seems to improve the miscibility of the OBC/PP blends at higher resin addition levels, but reduced the miscibility as the aromatic content of the resin increases. However, OBC/PE–PP blends showed improved miscibility with increasing aromatic content. A ternary phase morphology was particularly observed for both OBC/PP and OBC/PE–PP blends with highly aromatic (14%) unsaturated hydrocarbon resin, in which OBC formed the continuous phase, and PP, PE–PP, and unsaturated hydrocarbon resins formed the dispersed phase. Interestingly, we did not observe much difference in miscibility characteristics between the two saturated resin chemistries in both blend systems (OBC/PP and OBC/PE–PP). The Harkins spreading coefficient concept was used to better understand the ternary blend dispersed phase morphology. Spreading coefficients indicate that the free hydrocarbon resins (both unsaturated and saturated) were encapsulated by the amorphous PP or amorphous PE–PP polymer in the dispersed phase for the respective blend compositions. Overall OBC–PP and OBC/PE–PP blends showed better miscibility characteristics with both saturated aliphatic hydrocarbon resins, irrespective of the difference in resin chemistries. © 2013 Wiley Periodicals, Inc. J. Appl. Polym. Sci. 130: 2624–2644, 2013

KEYWORDS: blends; compatibilization; morphology; polyolefins; structure–property relations

Received 30 January 2013; accepted 16 April 2013; Published online 30 May 2013

DOI: 10.1002/app.39450

INTRODUCTION

Polyolefins are a very important class of polymers being used in a wide range of applications. Even though Carothers[1] reported different methods of producing polyolefins in the 1930s, the commercial production of polyolefins did not start until the 1940s when ICI introduced the high pressure polymerization process.[2] Further development of high quality commercial production of polyolefin materials started after the advent of olefin polymerization using the catalyst system introduced by Ziegler and Gellert[3] in 1950s, which resulted in the manufacture of linear polyethylene. The introduction of stereoregular polyolefin polymers by Natta[4] led to the development of a wide range of polyolefin polymer manufacturing including materials such as polypropylene and poly-1-butene. In 1970, Elaston[5] reported the synthesis of homogeneous, random, partially crystalline copolymers of ethylene and alpha-olefin. Until the late 1980s, Ziegler–Natta based catalyst chemistry dominated most of the commercial polyolefin manufacturing processes. Kaminsky[6] of Germany and Ewen[7] of EXXON chemicals reported the use of metallocene (zirconium) based catalyst systems to produce isotactic and syndiotactic polypropylene, respectively. This gas phase reaction technology provided higher comonomer incorporation with narrower molecular weight distribution. Later, Dow introduced a solution process using a metallocene based catalyst technology named constrained geometry catalysis technology, which enabled high activities for ethylene and

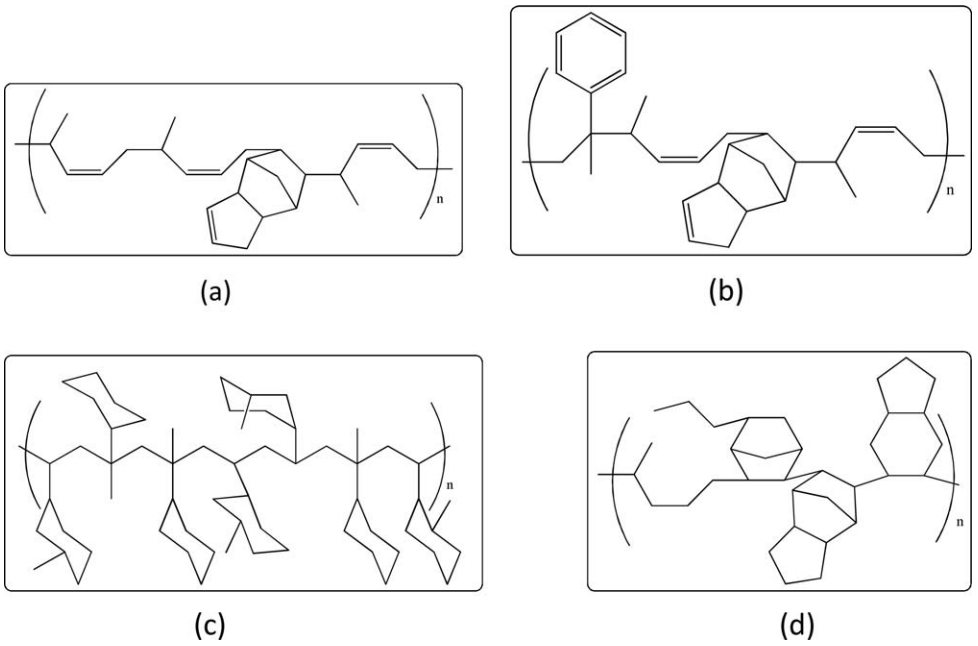

Figure 1. Ideal structures of a hydrocarbon resins. (a) An ideal unsaturated aliphatic C5 resin structure, (b) an ideal unsaturated aromatically modified aliphatic C5 resin structure, (c) an ideal saturated cycloaliphatic resin structure, and (d) an ideal saturated linear aliphatic–cycloaliphatic resin structure.

Table I. Properties of Polymers

Name	Penetration hardness (ASTM D5)	Viscosity (190°C) mPa S (ASTM D3236)	T_g (°C)
PP (propylene homopolymer)	18	2300	−10
PE–PP (ethylene–propylene copolymer)	35	5700	−20

alpha-olefin copolymerization, resulting in long chain branching and thus improved processablity.[8–10]

As can be seen, most of the developments in polyolefin polymer systems were based on new catalyst developments. Recently, in 2006, Arriola et al.[11] reported an olefinic block copolymer based on ethylene–octene, using a novel chain shuttling polymerization process. The chain shuttling catalyst technology promotes a "blocky" polymer structure that combines the attributes of high density polyethylene plastic and a polyolefin elastomer. Even though there have been several polyolefin based polymers, this polymer is of particular interest due to its similarity in rheological performance characteristics to the styrenic block copolymers used in hotmelt pressure-sensitive adhesive applications.[12–14] In 2007, Li Pi Shan et al.[14] first reported PSAs using high melt-index (15 and 21 at 190°C and 2.16 Kg) developmental olefinic block copolymers (OBCs) based on ethylene and octene. Even though these developmental OBCs had similar T_g as styrene–isoprene–styrene block copolymer (15 wt % styrene), they had comparably high G' with higher slope (temperature ramp) than styrene–isoprene–styrene block copolymer (15 wt % styrene). Thus the resulting PSA formulation with developmental OBCs showed high stiffness and required a significant amount of oil and tackifier, resulting in soft adhesive with inferior adhesive performance compared to the styrene–isoprene–styrene block copolymer (15 wt % styrene) based formulation.[14]

Recently, Dow has commercialized a 5 melt index (190°C, 2.16 Kg), 0.866 g/cm^3 density ethylene–octene based olefinic block copolymer (OBC). However, the G' for this OBC is still higher than the typical styrenic block co-polymer and correlates well with reported[14] developmental OBCs. We believe that blending this polymer with amorphous polyolefin polymers will increase the T_g and reduce the G', resulting in similar G' to a styrenic block copolymer. In this study, OBC blends with two APOs (PP

Table II. Polymer Blend Formulations in wt %

Formulation description	30/70 (OBC/PP)	50/50 (OBC/PP)	70/30 (OBC/PP)	30/70 (OBC/PE–PP)	50/50 (OBC/PE–PP)	70/30 (OBC/PE–PP)
OBC	30	50	70	30	50	70
PP	70	50	30	–	–	–
PE–PP	–	–	–	70	50	30

Table III. Properties of Hydrocarbon Resins

Resin	Type	Ring and ball softening point (°C)	% Aromatic content (^{1}H NMR)	Molecular weight $M_n/M_w/M_z$ (Daltons)
Unsaturated resins				
Resin 1 (R1)	Aliphatic	95	0.5	800/1700/3500
Resin 2 (R2)	Aliphatic/aromatic	95	5	850/2200/5500
Resin 3 (R3)	Aliphatic/aromatic	95	14	800/1700/4000
Saturated Resins				
Resin 4 (R4)	Cycloaliphatic	92	<0.1	500/700/1100
Resin 5 (R5)	Linear aliphatic–cycloaliphatic	100	<0.1	450/1000/2300

and PE–PP) were studied as potential base polymers for hotmelt pressure-sensitive adhesives. Second part of this study focuses on different compatibilization techniques using several hydrocarbon resins. Compatibilization techniques to improve the miscibility of polymer blend systems have been well studied. Extensive reviews, including several books on compatibilization of different polymer system already exist.[16–21] Compatibilizing agents improve the interfacial adhesion between the polymer system by reducing the interfacial tension. Compatibilizing agents can range from low molecular weight additives to high molecular weight polymers.[18] Hydrocarbon resin compatibilizers are of particular interest due to the fact that as early as 1845, natural or petroleum derived hydrocarbon resins are used to improve tack and processing characteristics of pressure-sensitive adhesives.[22–28] Hydrocarbon resins, also referred as tackifier resins are low molecular weight, high T_g, amorphous materials of petroleum origin. As Class and Chu explained,[25] a good tackifier resin should have low molecular weight, sufficient compatibility with polymer type, and have a glass transition temperature (T_g) higher than the base polymer to effectively impart sufficient pressure-sensitive adhesive characteristics such as tack and peel.[28] The hydrocarbon resins added to OBC/APO blends may not only modify individual phases or distribute between the different phases resulting in better miscibility, but also may improve the adhesive properties of the blends. One aliphatic unsaturated hydrocarbon resin (mainly based on piperylene or C5) and two aromatically modified C5 hydrocarbon unsaturated resins (styrene modified C5 hydrocarbon resin) with different aromatic content were selected for this study. One saturated cycloaliphatic hydrocarbon resin and one saturated linear aliphatic–cycloaliphatic hydrocarbon resin were also selected for this study to understand the effect of structural influence on the blend miscibility characteristics. These saturated cycloaliphatic and linear aliphatic–cycloaliphatic hydrocarbon resins are hydrogenated, low molecular weight, high T_g amorphous materials. Hydrocarbon resins evaluated in this study are derived from crude petroleum feedstock. The simplified structure given in Figure 1 is an idealized structure, rather than a particular actual one.

Influence of hydrocarbon resins on the effect of morphology (phase modification) and viscoelastic properties have been

Table IV. OBC–PP–Resins Blend Formulations in wt %

Formulation description	OBC	PP	Resin 1 (R1)	Resin 2 (R2)	Resin 3 (R3)	Resin 4 (R4)	Resin 5 (R5)
40/40/20 (OBC/PP/R1)	40	40	20	–	–	–	–
35/35/30 (OBC/PP/R1)	35	35	30	–	–	–	–
30/30/40 (OBC/PP/R1)	30	30	40	–	–	–	–
40/40/20 (OBC/PP/R2)	40	40	–	20	–	–	–
35/35/30 (OBC/PP/R2)	35	35	–	30	–	–	–
30/30/40 (OBC/PP/R2)	30	30	–	40	–	–	–
40/40/20 (OBC/PP/R3)	40	40	–	–	20	–	–
35/35/30 (OBC/PP/R3)	35	35	–	–	30	–	–
30/30/40 (OBC/PP/R3)	30	30	–	–	40	–	–
40/40/20 (OBC/PP/R4)	40	40	–	–	–	20	–
35/35/30 (OBC/PP/R4)	35	35	–	–	–	30	–
30/30/40 (OBC/PP/R4)	30	30	–	–	–	40	–
40/40/20 (OBC/PP/R5)	40	40	–	–	–	–	20
35/35/30 (OBC/PP/R5)	35	35	–	–	–	–	30
30/30/40 (OBC/PP/R5)	30	30	–	–	–	–	40

Table V. OBC–(PE–PP)–Resin Blend Formulations in wt %

Formulation description	OBC	PE–PP	Resin 1 (R1)	Resin 2 (R2)	Resin 3 (R3)	Resin 4 (R4)	Resin 5 (R5)
40/40/20 (OBC/PE–PP/R1)	40	40	20	–	–	–	–
35/35/30 (OBC/PE–PP/R1)	35	35	30	–	–	–	–
30/30/40 (OBC/PE–PP/R1)	30	30	40	–	–	–	–
40/40/20 (OBC/PE–PP/R2)	40	40	–	20	–	–	–
35/35/30 (OBC/PE–PP/R2)	35	35	–	30	–	–	–
30/30/40 (OBC/PE–PP/R2)	30	30	–	40	–	–	–
40/40/20 (OBC/PE–PP/R3)	40	40	–	–	20	–	–
35/35/30 (OBC/PE–PP/R3)	35	35	–	–	30	–	–
30/30/40 (OBC/PE–PP/R3)	30	30	–	–	40	–	–
40/40/20 (OBC/PE–PP/R4)	40	40	–	–	–	20	–
35/35/30 (OBC/PE–PP/R4)	35	35	–	–	–	30	–
30/30/40 (OBC/PE–PP/R4)	30	30	–	–	–	40	–
40/40/20 (OBC/PE–PP/R5)	40	40	–	–	–	–	20
35/35/30 (OBC/PE–PP/R5)	35	35	–	–	–	–	30
30/30/40 (OBC/PE–PP/R5)	30	30	–	–	–	–	40

investigated in this study. Even though there have been several studies and reviews[2,15,20] of polyolefin blends for the improvement of different properties and processing characteristics, there has not been any known reported literature describing blends of OBCs and APOs.

MATERIALS AND METHODS

A commercially available (INFUSE 9507) 5 melt index (190°C, 2.16 Kg), 0.866 g/cm^3 density ethylene–octene based olefinic block copolymer (OBC) was obtained from Dow Chemical Company. Atactic propylene homopolymer amorphous polyolefin and ethylene–propylene amorphous polyolefin copolymers were obtained from Eastman Chemical Company. Properties of the amorphous polyolefins (atactic propylene homopolymer and ethylene–propylene copolymer) are given in Table I.

Blends containing a 30, 50, and 70 wt % OBC with PP or PE–PP were prepared using a Plasticorder Brabender at 150°C using roller blades. The formulations were blended for 20–45 min until the torque became constant (to ensure proper mastication and homogenous blending). The OBC/APO formulations evaluated are given in Table II. Properties of hydrocarbon resins (compatibilizing agent) is given in Table III. Hydrocarbon resins were supplied by Eastman Chemical Company. OBC/PP/Resin Formulations evaluated are given in Table IV and OBC/PE–PP/Resin Formulations evaluated are given in Table V.

Ring and Ball Softening Point of hydrocarbon resin was measured using the Herzog Ring and Ball Tester. The softening point is defined as the temperature at which a disk of the sample held within a horizontal ring is forced downward a distance of 25.4 mm (1 inch) under the weight of a steel ball as the sample is heated at 5°C/min in a silicon bath (400 mL). The temperature is recorded, when the resin sample passes through the sensors of the unit (ASTM D-6493-99).

To determine the aromatic hydrogen content of each hydrocarbon resin, the ratio of the integration area of aromatic hydrogen relative to the total integration area of hydrogen on the resin's NMR spectrum was determined via ^{1}H NMR analysis. The NMR analysis was performed using a JEOL 600 MHz Eclipse NMR system with a pulse interval of 15 s, acquisition time of 3.6 s, pulse angle of 90°, X resolution of 0.27 Hz, and number of scans set at 16. The resin NMR samples were prepared by dissolving a known amount of each of hydrocarbon resins in methylene chloride-d2. The total integration value was normalized to 100. The results were reported in area percent.

Molecular weights (M_n, M_w, and M_z) of hydrocarbon resins were determined via gel permeation chromatography (GPC) with THF as a solvent. Each resin was analyzed at ambient temperature in Burdick and Jackson GPC-grade THF stabilized with BHT, at a flow rate of 1 mL/min. Sample solutions were prepared by dissolving about 50 mg of each resin in 10 mL of THF and adding 10 μL of toluene thereto as a flow-rate marker. An auto sampler was used to inject 50 μL of each solution onto a Polymer Laboratories PLgel^{TM} column set consisting of a 5 μm Guard, a Mixed-C^{TM} and an Oligopore^{TM} column in series. The eluting polymer was detected by differential refractometry, with the detector cell held at 30°C. The detector signal was recorded by a Polymer Laboratories Caliber^{TM} data acquisition system, and the chromatograms were integrated with software developed at Eastman Chemical Company. A calibration curve was determined with a set of 18 nearly monodisperse polystyrene standards with molecular weight from 266 to 3,200,000 g/mol and 1-phenylhexane at 162 g/mol. The molecular weight distributions and averages were reported either as equivalent polystyrene values.

Surface tension measurements of hydrocarbon resins and polymers were obtained through contact angle measurements. Contact angle measurements were performed using VCA2500 XE video contact angle system (AST Products Inc. MA). Contact

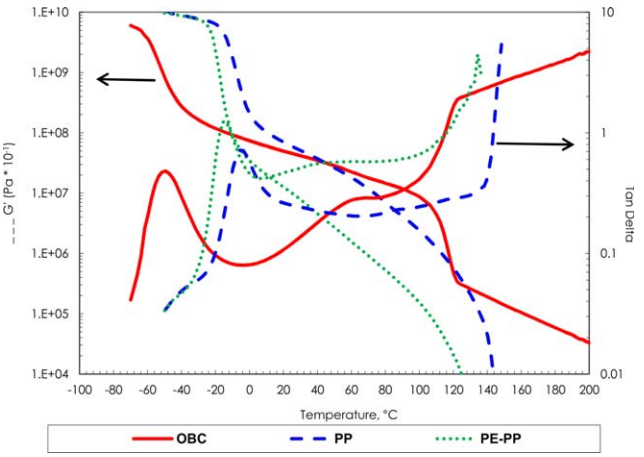

Figure 2. DMA plots for OBC, PP, and PE–PP polymers. [Color figure can be viewed in the online issue, which is available at wileyonlinelibrary.com.]

angle measurements were performed on a 0.5 mil thick coated film of hydrocarbon resins and polymers on a glass plate. Contact angle of the solid surface with two liquids of known surface energy (distilled water and methylene iodide) was used to obtain the information about the surface free energy of the solid substrate. A sessile drop of liquid (distilled water followed by methylene iodide) was placed on the coated glass substrate surface. This created a specified contact (tangent) angle at the solid, liquid, air interface. A photograph of the drop profile was used to calculate the contact angle. Calculations of the wetting parameters were derived from thermodynamic principles based on Young's equation, which describes the stable equilibrium at a three-phase boundary between a solid, liquid, and a vapor system (VCA software). Surface energy calculations were performed using Harmonic calculation with the help of SE2500 software.

A 1 : 1 polymer blend ratio of OBC/APO (where the APO is either PP or PE–PP) was selected for this study to better understand the influence of resin addition in three different levels 20, 30 and 40 wt %.

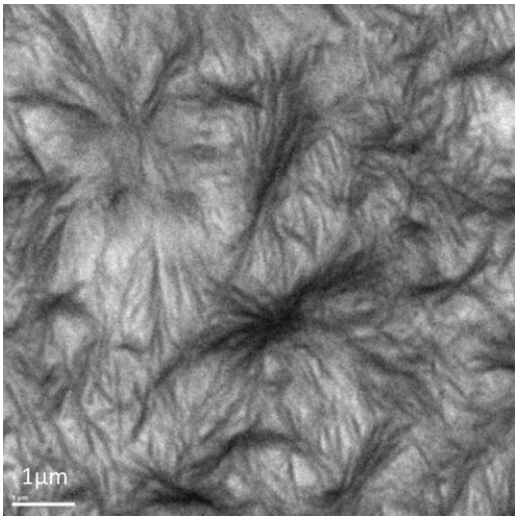

Figure 3. TEM micrograph of the OBC polymer.

Compatibility and polymer miscibility of the blends was evaluated using Dynamic Mechanical Analysis (DMA) and morphology of the blends was analyzed using Transmission Electron Microscopy (TEM). There have been several reports describing the effectiveness of determining the polymer compatibility and miscibility characteristics of polymer blends using dynamic mechanical analysis and describing morphological analysis using microscopic techniques.[20,21,29–31]

Dynamic Mechanical Analysis (DMA) of the blends was performed using a TA Instruments Ares RDA3® Rheometer in a parallel plate geometry. The diameter of the plates was 8 mm and the gap was set at 2.33 mm. Temperature sweep experiment was performed between −80 and 300°C with a heating rate of 6°C/min, by keeping the frequency at 10 Hz and the maximum strain at 5%.

TEM images were taken after the blends were microtomed into 50 nm thickness using a Leica EM UC6 cryo-microtome with a knife temperature at −110°C and sample temperature at −120°C. These thin sections were then transferred onto TEM grids. TEM evaluation was performed using a Philips CM12 Microscopy with an accelerating voltage of 100 kV. No chemical staining has been applied to the sections. The contrast in the images is mainly created by density differences between the different structures.

RESULTS AND DISCUSSION

Evaluation of OBC/APO Blends

OBC/PP blends will be discussed first followed by OBC/PE–PP blends. Figure 2 shows the viscoelastic characteristics of OBC, PP, and PE–PP polymers. As can be seen from the tan δ peak of Figure 2, the OBC copolymer shows a T_g of −49°C. PE–PP copolymer has a lower T_g and lower modulus than that of the PP homopolymer. The storage modulus (G') of OBC at room temperature (25°C) is higher than that of PE–PP amorphous polymer, but little lower compared to PP homopolymer. Even though the elastic modulus of OBC decreases as the temperature increases, the decrease is not as pronounced as for the PP and PE–PP polymers. This shows the lack of elastic properties (strength) for PP and PE–PP polymers compared to OBC. Therefore PP and PE–PP polymers cannot be used as such for pressure-sensitive adhesives (PSA) applications due to the lack of elastic strength needed over a wide application temperature range, before it starts to flow. Morphological characterizations of the polymers were also evaluated using TEM. Figure 3 shows the TEM micrographs of the polymer.

The dark crystalline regions and light amorphous regions of OBC are clear from Figure 3. The dark lamellar worm like regions correspond to crystalline domains embedded in a light continuous amorphous matrix. Unfortunately, due to predominant amorphous characteristics of PP and PE–PP amorphous polymers, it was unable to obtain good TEM micrographs, since they formed transparent films due to the lack of heterogeneity or phase contrast. As mentioned earlier, the G' for this OBC is still higher than the typical styrenic block co-polymer used in PSA applications.[14] Therefore OBC/PP and OBC/PE–PP blends were prepared to reduce the elastic modulus of OBC polymer.

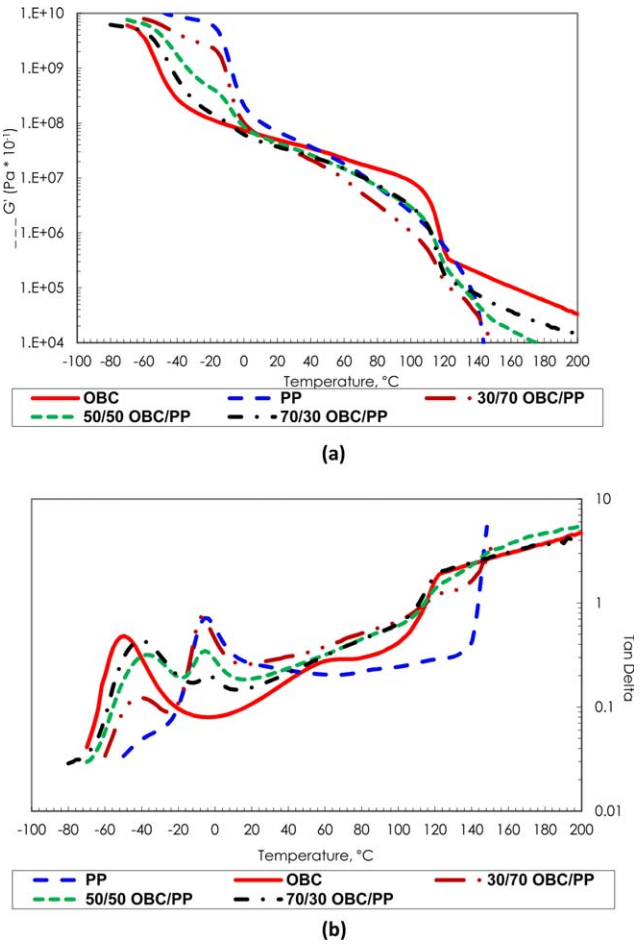

Figure 4. DMA plots for the OBC/PP blends: (a) storage modulus and (b) Tan δ. [Color figure can be viewed in the online issue, which is available at wileyonlinelibrary.com.]

Figure 4 shows the viscoelastic characteristics of OBC/PP blends at three different ratios as specified in Table II.

It is clear from Figure 4 that the OBC/PP blends show two tan delta peaks (two glass transitions) at 30, 50, and 70% addition levels, which is a clear indication of immiscibility. There is a first transition around −40°C and a second transition around −10°C. The second glass transition for 30/70 OBC/PP corresponds to the PP glass transition temperature. All three blends show similar second glass transition temperatures (T_g) as for the parent PP homopolymer. While the first glass transition for all three blends are almost 10°C higher than that of the parent OBC polymer. The change in the first thermal transition associated with the OBC is an indication of limited miscibility of the PP homopolymer in OBC matrix. Tan delta peak height also correlate with the level of OBC and PP in the blend. Morphological characterization of the OBC/PP blends was also evaluated using TEM. Figure 5 shows the TEM micrographs of the OBC/PP blends.

As can been seen from the above TEM micrographs (Figure 5), all the blends show a two phase blend morphology. Immiscibility of the blends is very obvious. It can be observed that at 30 wt % OBC addition level, OBC forms the dispersed phase (Dark worm-like regions) and PP forming the continuous phase, but as the OBC concentration in the blend increases to 50 wt %, phase inversion happens resulting in OBC matrix forming the continuous phase and the PP polymer forming the dispersed phase of the blend morphology. At 50 and 70 wt % APO addition level, the amount of dispersed phase increases as the amount of amorphous polyolefin content increases. Even though we can see some dark crystalline phases of OBC, they are not as well defined as for the OBC homopolymer, indicating some loss of crystalline architecture. This is more pronounced as the amount of PP increases in the blend composition (50 and 70 wt %).

Figure 6 shows the viscoelastic characteristics of OBC/PE–PP blends. OBC/PE–PP blends also show similar glass transition behaviors as for OBC/PP blends. It is interesting to note that the elastic modulus of the blends show a different behavior for OBC/PE–PP blends. In this case, the elastic modulus at room temperature gradually decreases as the amount of PE–PP amorphous polymer increases in the blend. The 50/50 OBC/PE–PP polymer blend shows an elastic modulus (at room temperature) in the middle of the respective OBC and PE–PP polymers, indicating some miscibility between the polymers.

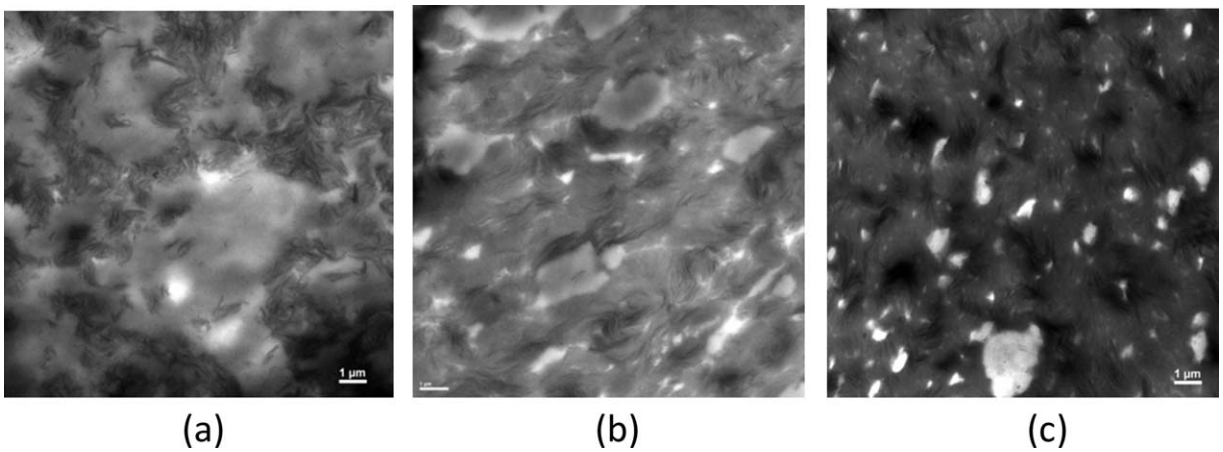

Figure 5. TEM micrographs of OBC/PP blends: (a) 30/70 OBC/PP, (b) 50/50 OBC/PP, and (c) 70/30 OBC/PP.

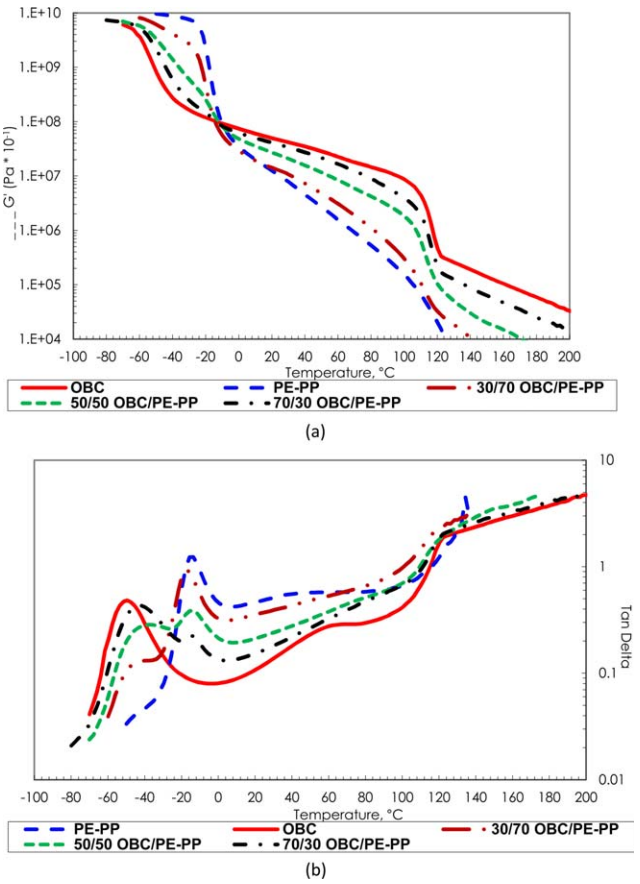

Figure 6. DMA plots for the OBC/PE–PP blends: (a) storage modulus and (b) Tan δ. [Color figure can be viewed in the online issue, which is available at wileyonlinelibrary.com.]

Morphological evaluation of the OBC/PE–PP blends was also performed and can be seen in Figure 7. As discussed earlier in the case of OBC/PP polymer, OBC/PE–PP (Figure 7) also shows a two-phase morphology. At 30 wt % OBC addition level, OBC forms the dispersed phase and PE–PP forming the continuous phase. However, as the OBC concentration increases to 50 wt %, the phase inversion happens, resulting in OBC becoming the continuous phase and the PE–PP amorphous polymer forming the dispersed phase. It has been learned that

- Both OBC/PP blends and OBC/PE–PP show two glass transitions at 30, 50, and 70% addition levels. In both cases, the glass transition temperatures correspond to their parent polymers, which is a clear indication of incompatibility.
- Interestingly, the elastic modulus (at room temperature) of OBC/PE–PP blends decreased as the amount of PE–PP amorphous polymer increased in the blend and was in between both the parent polymers, indicating some interaction between the polymer phases. On the other hand for OBC/PP blends, the elastic modulus (at room temperature) was a little lower than that of the two parent polymers, but did not show a significant effect on modulus (G') indicating no interaction between the phases.
- Morphological evaluation of both blends (OBC/PP and OBC/PE–PP) again verified the immiscibility characteristics of the blends. In case of both blends (OBC/PP and OBC/PE–PP), it has been observed that at 30 wt % OBC addition level, OBC forms the dispersed phase, but as the OBC concentration in the blend increases to 50 wt %, phase inversion happens resulting in OBC matrix forming the continuous phase and the PP polymer or the PE–PP polymer forming the dispersed phase of the blend morphology, respectively. At 50 and 70 wt % APO addition level, the amount of dispersed phase increased as the amount of amorphous polyolefin content increased.

Since OBC/PP and OBC/PE–PP polymer blends were immiscible, each exhibiting the T_g of pure blend components and a heterogeneous morphology, a compatibilizing agent is needed to improve the miscibility characteristics of the polymer system. The effect of different low molecular weight hydrocarbon resins was evaluated as compatibilizing and tackifying agents to improve the interfacial adhesion (miscibility) characteristics between the two polymers. The next two sections describe the effect of five different hydrocarbon resins with different chemistries as compatibilizing agents.

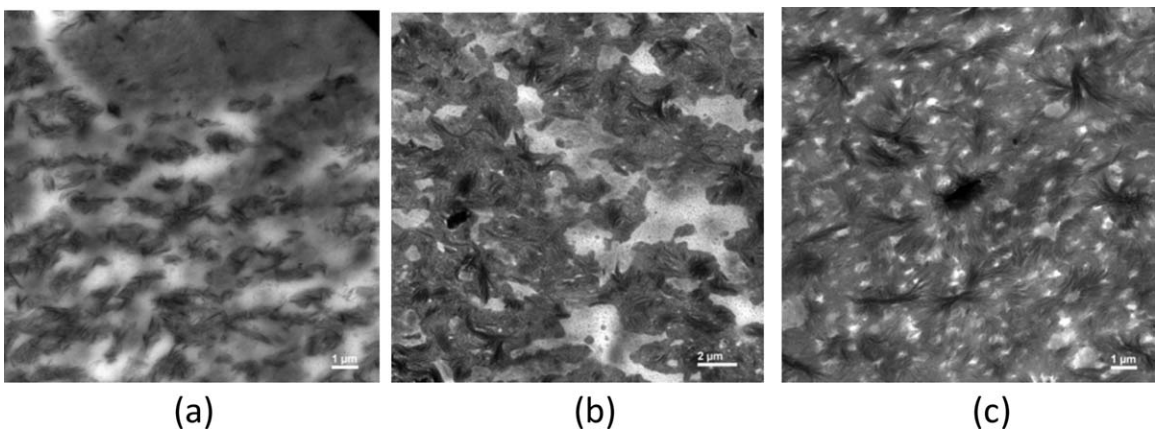

Figure 7. TEM micrographs of OBC/PE–PP blends: (a) 30/70 OBC/PE–PP, (b) 50/50 OBC/PE–PP, and (c) 70/30 OBC/PE–PP.

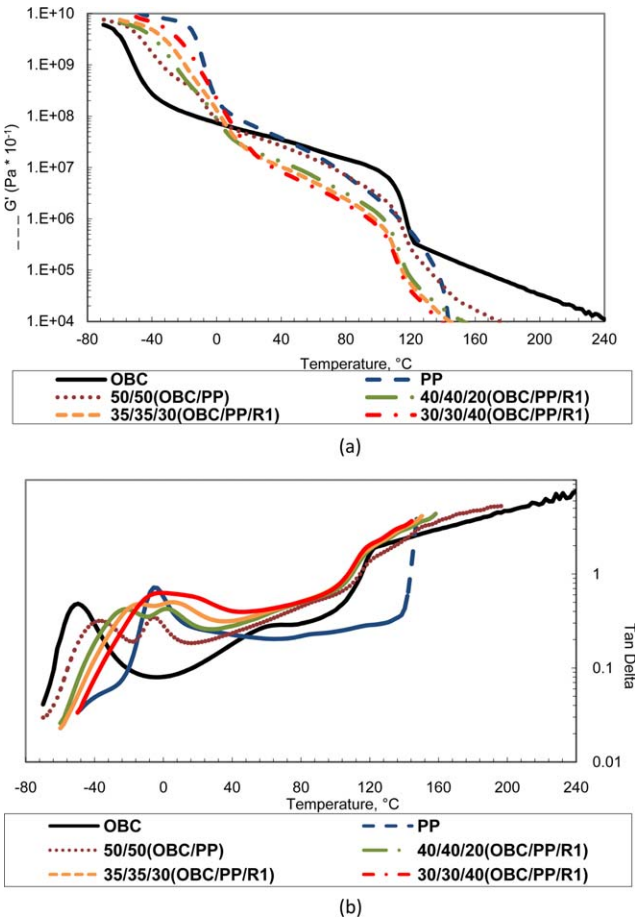

Figure 8. DMA of OBC/PP/Aliphatic unsaturated resin blends at different ratios: (a) storage modulus and (b) Tan δ. [Color figure can be viewed in the online issue, which is available at wileyonlinelibrary.com.]

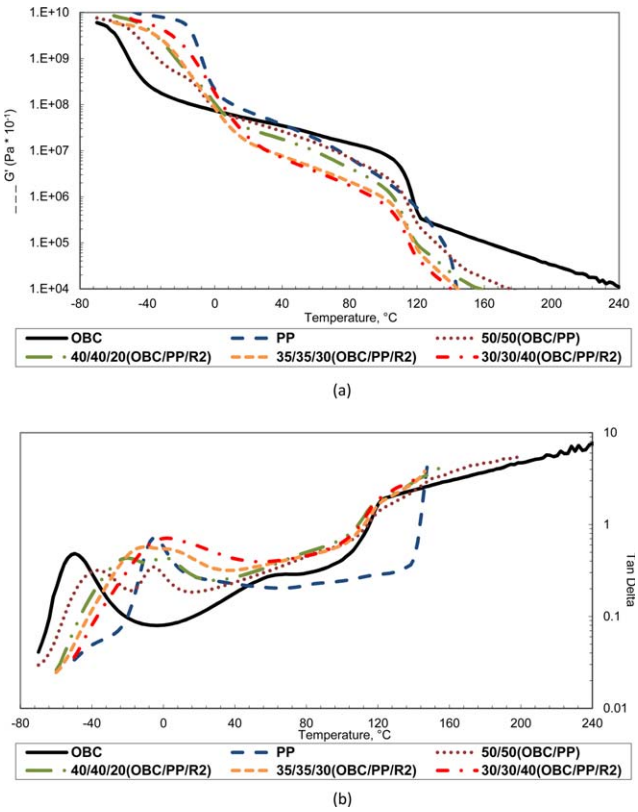

Figure 9. DMA of OBC/PP/aliphatic–aromatic (5%) resin blends at different ratios: (a) storage modulus and (b) Tan δ. [Color figure can be viewed in the online issue, which is available at wileyonlinelibrary.com.]

Effect of Unsaturated Hydrocarbon Resins on OBC/APO Blends

Viscoelastic properties measured using dynamic mechanical analysis (DMA) of the OBC/PP blends and OBC/PE–PP blends with different hydrocarbon resins are discussed in the first part, followed by morphological evaluation (TEM) of the OBC/PE–PP blends and OBC/PE–PP blends with different hydrocarbon resins. Dynamic mechanical analysis of the OBC/PP blends with aliphatic resin (Resin 1) at three different concentrations is shown in Figure 8.

It can be seen from the above viscoelastic properties that both 20 and 30 wt % additions of aliphatic unsaturated resin (R1) still show two glass transitions indicating immiscibility. However 40 wt % addition of aliphatic unsaturated resin shows a single, broad glass transition temperature. It should be noted that the first glass transition temperature and the second glass transition temperature significantly increased for the blends containing 20 and 30 wt % aliphatic unsaturated resin (R1) indicating good miscibility of the resin in individual polymer phases. The glass transition temperature for the 40 wt % aliphatic unsaturated resin containing blend is close to that of PP polymer and shows a broad tan δ peak. Elastic modulus (G') decreases as the amount of unsaturated aliphatic resin in the blend increases. This is an indication of better miscibility as the aliphatic unsaturated resin concentration increases.

Figure 9 shows the viscoelastic characteristics of OBC/PP blends containing aliphatic–aromatic (5%) resin (R2) at different concentrations. This also follows the same trend as it has seen for the aliphatic unsaturated resin containing blends. Interestingly 40 wt % aliphatic–aromatic (5%) resin containing blends show a single glass transition, indicating miscibility similar to 40 wt % aliphatic resin blend. The lower elastic modulus of 40 wt % aliphatic–aromatic (5%) resin containing blends is also an indication of good miscibility of the different phases. Figure 10 shows the viscoelastic characteristics of aliphatic–aromatic (14%) resin containing OBC/PP blend.

From Figure 11, as the amount of resin increases, the total aromatic content in the formulation also increases, resulting in immiscibility even at 40 wt % addition levels. Also, as the amount of resin increases, T_g of the total formulation increases and the elastic modulus (G') of the formulation decreases. This is an indication of partial miscibility of the different phases, but it is not as good as with aliphatic unsaturated resin and aliphatic–aromatic (5%) resin containing blends.

Figure 11 shows the effect of aromatic content at 40 wt % addition levels for the unsaturated resin containing OBC/PP blends. In Figure 11, 5% aromatic–aliphatic resin at 40 wt % addition level shows better miscibility characteristics (higher T_g, single tan δ curve, and lower elastic modulus) compared to

Applied Polymer SCIENCE

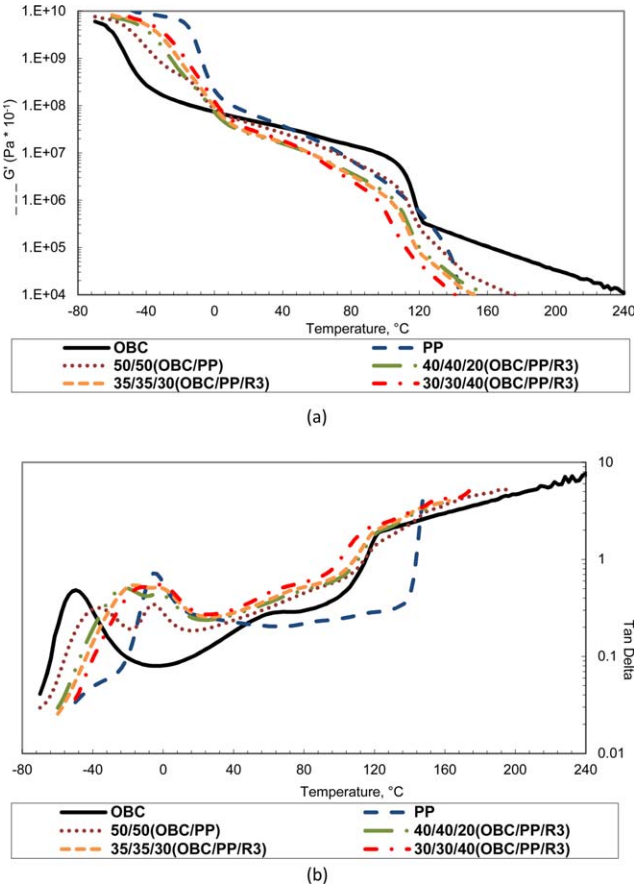

Figure 10. DMA of OBC/PP/aliphatic–aromatic (14%) unsaturated resin blends at different ratios (a) storage modulus and (b) Tan δ. [Color figure can be viewed in the online issue, which is available at wileyonlinelibrary.com.]

aliphatic–aromatic (14%) resins (R3). We expected the aliphatic resin (R1) to show better miscibility due to the structural similarity in resin composition with ethylene–octene based OBC and polypropylene amorphous polymer blends.

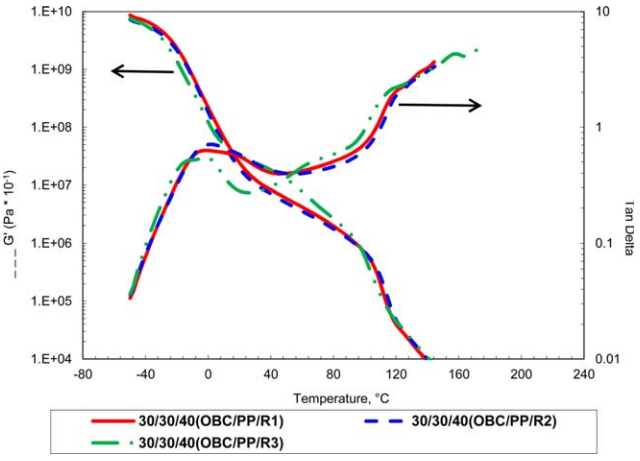

Figure 11. DMA of 40 wt % unsaturated resin containing OBC/PP blends with increasing resin aromatic content. [Color figure can be viewed in the online issue, which is available at wileyonlinelibrary.com.]

Interestingly a small amount of aromatic content (5%) actually shows similar or slightly improved miscibility of OBC/PP blends compared to blends containing aliphatic unsaturated resin (R1). Figure 12 shows the ternary plot of OBC/PP blends with unsaturated hydrocarbon resins, binary blends of OBC with unsaturated hydrocarbon resins and binary blends of PP with unsaturated hydrocarbon resins. The bottom axis represents the amount of PP, and the circular dots represent the T_g of particular binary blends of PP with unsaturated hydrocarbon resins. The axis on the left is the amount of OBC. Axis on the right of the ternary plot represents the amount of hydrocarbon resin, and the circular dots represent the T_g of particular binary blends of OBC with hydrocarbon resins. Ternary blend T_g is represented as circular dots in the middle of the ternary plot where the OBC, PP, and amounts of each particular hydrocarbon resin intersects with respect to the corresponding blend ratios.

Blackened dots indicate blends with two T_g's and clear dots indicate blends with a single T_g. The amount of resin concentration was kept the same (20, 30, and 40 wt %) for binary blends of polymers (OBC or PP) with hydrocarbon resins, (R1, R2, and R3), as for the ternary blends (two polymers with resin). In Figure 12, binary blends of OBC polymer with any of the hydrocarbon resins shows a single T_g, and the aromatic content of resin has little effect on the compatibility. However, binary blends of PP with hydrocarbon resins show a completely different behavior such that as the aromatic content in the resin increases, the incompatibility also increases, resulting in two T_g's at all concentrations of resin for the PP-R3 blends. Figure 13 below shows the effect of aliphatic hydrocarbon resin in OBC/PE–PP blends at three different ratios.

From Figure 13, 30 and 40 wt % addition of aliphatic hydrocarbon resin to the OBC/PE–PP blends show a single glass transition temperatures and higher glass transition temperatures than that of the parent polymers. It is interesting to note that the storage modulus (G', at room temperature) of the 20, 30, and 40 wt % aliphatic hydrocarbon resin containing OBC/PE–PP blends show a similar trend and is in between the individual polymer values and lower than the 50/50 OBC/PE–PP blend without any resin. This behavior is different than that of the OBC/PP blends containing aliphatic hydrocarbon resins (Figure 8), in which the blends containing resins showed lower modulus than that of the parent polymers. The G' values (at room temperature) in between the parent polymer show better miscibility between the interphase of the two polymer system, while the very low storage modulus (G', at room temperature) lower than the two parent polymers, and especially PP, shows that the resin is softening the PP phase more than that of the OBC/PP interphase. Figure 14 shows the viscoelastic properties of aliphatic–aromatic (5%) hydrocarbon resin containing OBC/PE–PP blend at different resin concentrations.

Interestingly aromatically modified aliphatic resins improve the miscibility characteristics of the OBC/PE–PP blends, even at low resin addition amount (20 wt %) as can be seen in Figure 14. As the resin amount increases, the miscibility also improves resulting in single glass transition at 30 and 40 wt % resin

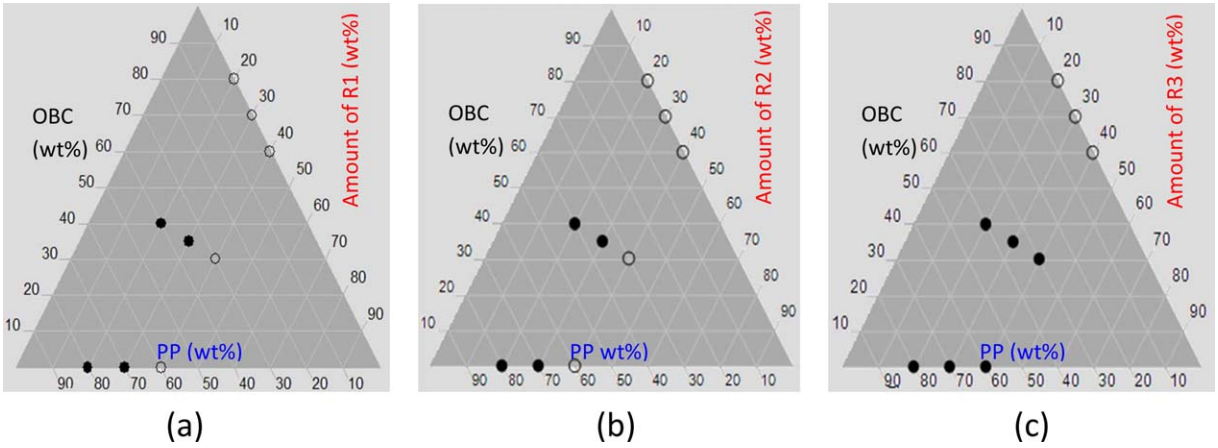

Figure 12. Ternary plot of glass transition temperatures for OBC/PP blends with resins. (a) Resin 1 (R1), (b) Resin 2 (R2), and (c) Resin 3 (R3). [Color figure can be viewed in the online issue, which is available at wileyonlinelibrary.com.]

addition. The elastic modulus also decreases as the aromatic resin amount increases and is in between both parent polymers and the 50/50 OBC/PE–PP blends. Figure 15 shows the highly aromatic (14%), aliphatic–aromatic unsaturated resin effect in OBC/PE–PP blends.

As mentioned earlier, higher aromatic content actually has definite influence in miscibility characteristics of OBC/PE–PP blends. A 20, 30, and 40 wt % resin addition amounts of 14% aromatic resin addition to OBC/PE–PP blends shows a single T_g, narrower tan δ curve, and lower elastic modulus

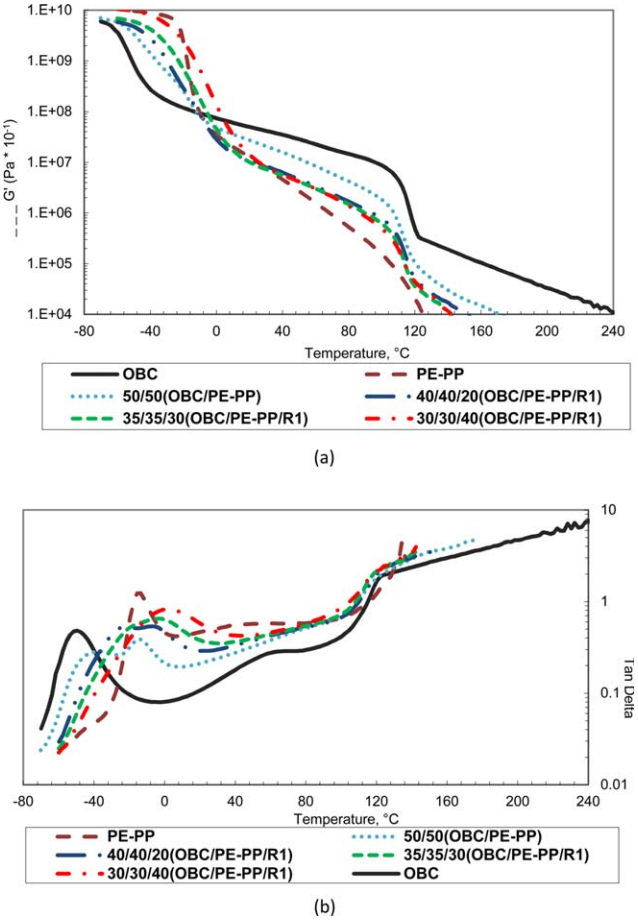

Figure 13. DMA of OBC/PE–PP/aliphatic unsaturated resin blends at different ratios: (a) storage modulus and (b) Tan δ. [Color figure can be viewed in the online issue, which is available at wileyonlinelibrary.com.]

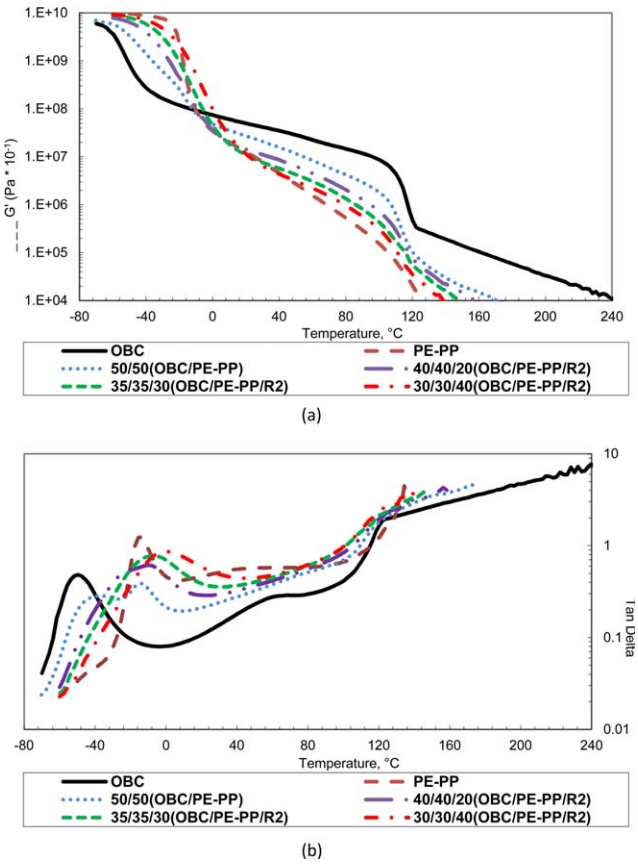

Figure 14. DMA of OBC/PE–PP/aliphatic–aromatic (5%) unsaturated resin blends at different ratios: (a) storage modulus and (b) Tan δ. [Color figure can be viewed in the online issue, which is available at wileyonlinelibrary.com.]

Applied Polymer SCIENCE

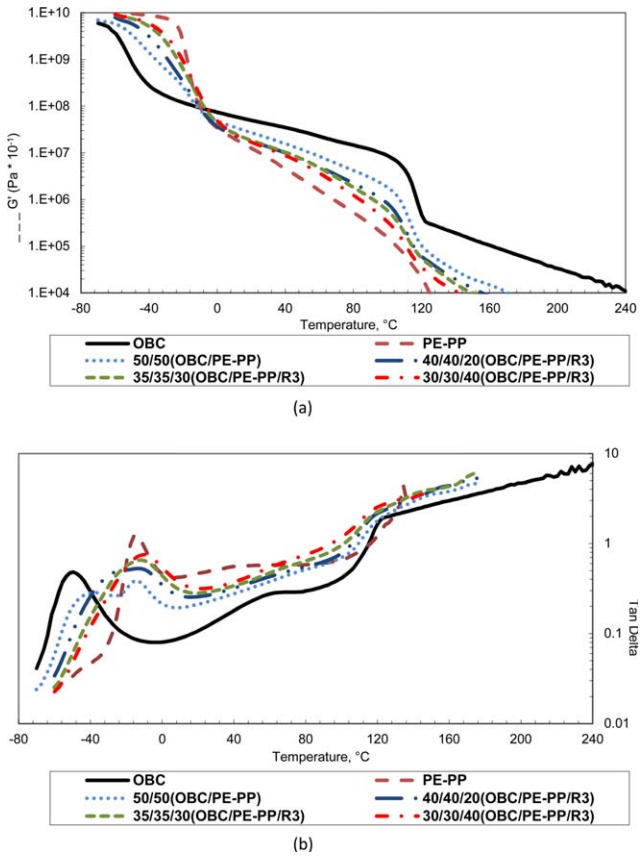

Figure 15. DMA of OBC/PE–PP/aliphatic–aromatic (14%) unsaturated resin blends at different ratios: (a) storage modulus and (b) Tan δ. [Color figure can be viewed in the online issue, which is available at wileyonlinelibrary.com.]

characteristics, likely indicating improved miscibility. It is interesting to note that higher aromatic content resin addition to OBC/PP blends showed very poor miscibility characteristics. However, in the case of OBC/PE–PP blends with higher aromatic content resin (14%), aromatic content seems to improve the miscibility behavior. Approximately 8% ethylene content in PE–PP polymer seems to improve the interfacial miscibility

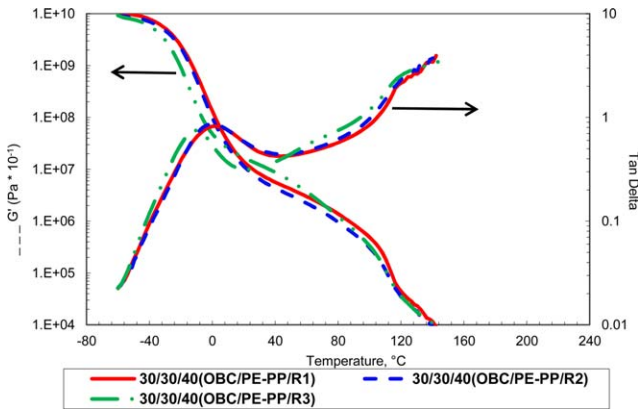

Figure 16. DMA of 40 wt % unsaturated resin containing OBC/PE–PP blends with increasing resin aromatic content. [Color figure can be viewed in the online issue, which is available at wileyonlinelibrary.com.]

characteristics of OBC/PE–PP blend, when formulated with an aliphatic–aromatic resin. Figure 16 shows the influence of unsaturated resin aromatic content on OBC/PE–PP blend.

As can be seen (Figure 16), the higher aromatic content (14%) resin addition at 40 wt % level to OBC/PE–PP blends results in a single tan δ peak, indicating better miscibility between the blend components, compared to the lower aromatic content (5%) resin (R2) and aliphatic unsaturated resin (R1). Figure 17 shows the ternary plot of OBC/PE–PP blends with hydrocarbon resins, binary blends of OBC with unsaturated hydrocarbon resins and binary blends of PE–PP with hydrocarbon resins. Bottom axis represents the amount of PE–PP, and the circular dots represent the T_g of particular binary blends of PE–PP with hydrocarbon resins. The axis on the left corresponds to the amount of OBC. The axis on the right of the ternary plot represents the amount of unsaturated tackifier resin, and the circular dots represent the T_g of the particular binary blends of OBC with hydrocarbon resins. Ternary blend T_g is represented as circular dots in the middle of the ternary plot where the OBC, PE–PP, and amounts of particular tackifier intersects with respect to the corresponding blend ratios. Blackened dot indicates blends with two T_g's and the clear dot indicates blends with a single T_g. The amount of resin concentration was kept the same (20, 30, and 40 wt %) for binary blends of polymers (OBC or PP with unsaturated hydrocarbon resins, R1, R2, and R3), as for the ternary blends (two polymers with resin). In Figure 17, binary blends of OBC polymer with all three hydrocarbon resins shows a single T_g, and the aromatic content of the resin has little effect on the compatibility. Interestingly, binary blends of PE–PP with hydrocarbon resins also show a single T_g, and the aromatic content of the resin has little effect on the compatibility, which is a completely different behavior than that of the PP-resin blends, which showed two T_g's at higher polymer concentration levels (in the blends) and also with aromatic content of the resin. It should be noted that the polyethylene containing polymer shows better miscibility characteristics with hydrocarbon resins, irrespective of the aromatic content, which is evident from an OBC polymer stand point (which is an ethylene–octene polymer) and the PE–PP amorphous polyolefin stand point. The rigid backbone of PP with a bulky methyl group, compared to the more flexible linear polyethylene backbone, could help explain the differences we see in the miscibility behaviors for the blends.

Polymer miscibility characteristics can be further verified by observations through electron microscopy. In this study, Transmission Electron Microscopy (TEM) was employed to better understand the miscibility behavior of the OBC/PP and OBC/PE–PP blends with different hydrocarbon resins. Figure 18 shows the TEM micrographs of OBC/PP blends containing three different hydrocarbon resins. The continuous phase and dispersed phase morphologies of the OBC/PP containing unsaturated resin blends are clear from the above TEM micrographs. TEM micrographs in rows represent the increasing amount of same unsaturated resin in the blend, while the TEM micrographs in columns represents the higher amount of aromatic content in ascending order at the same resin addition levels. The dark areas represent the OBC polymer phase containing

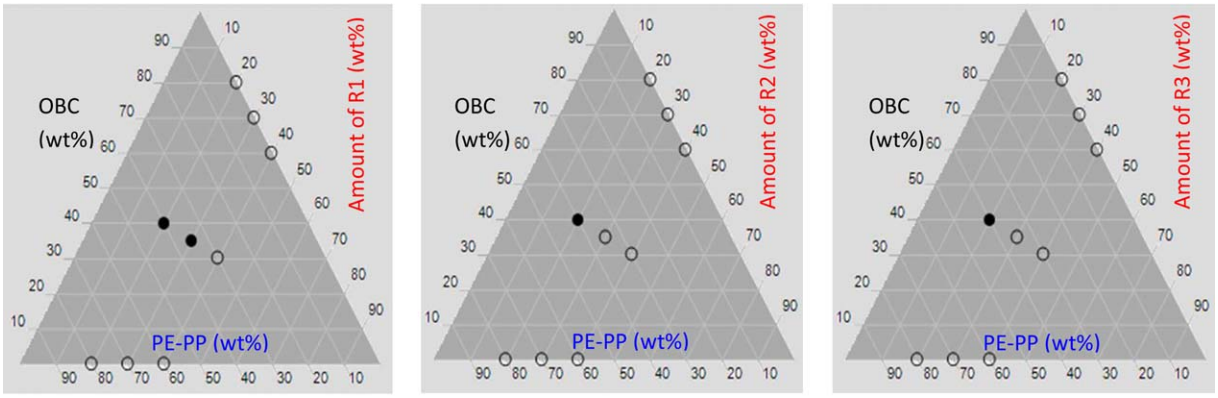

Figure 17. Ternary plot of glass transition temperatures for OBC/PE–PP blends with resins. (a) Resin 1 (R1), (b) Resin 2 (R2), and (c) Resin 3 (R3). [Color figure can be viewed in the online issue, which is available at wileyonlinelibrary.com.]

resin, and the light dispersed phase is the PP with resin. Since it was difficult to selectively stain one of the phases due to the chemical nature of the blend components, the phase contrast is due to density differences. Improved miscibility of the 40 wt % aliphatic unsaturated resin (R1) containing OBC/PP blend can be correlated well to the single T_g observed from DMA (Figure 8), compared to the other two lower addition levels. Improved miscibility can be also seen with 30 and 40 wt % addition of slightly aromatic (5%) aliphatic-aromatic resin (R2) containing OBC/PP blend, and can be correlated well to the single glass transition observed (Figure 10). However, high aromatic content (14%) unsaturated resin (R3) containing OBC/PP blend clearly shows the well-dispersed dark aromatic resin phase along with light PP-resin phase. Dispersion sizes appear to be going from 1 micron to 3 microns. Slight immiscibility behavior of the OBC/PP blend containing highly aromatic (14%) aliphatic–aromatic unsaturated resin can also be correlated to the two different glass transition temperatures observed at all three addition levels (Figure 10).

Phase morphologies of OBC/PE–PP blends (Figure 19) with hydrocarbon resins are similar to that of OBC/PP blends with hydrocarbon resins, in which the OBC–resin matrix forms the continuous phase while the PE–PP–resin matrix forms the dispersed phase. The continuous and dispersed phase morphologies of the blends containing aliphatic unsaturated resin (R1) containing blends and slightly aromatic (5%) aliphatic–aromatic resin (R2) containing OBC/PE–PP blend is obvious in the case of 20 wt % addition levels. At 30 and 40 wt % addition levels, even though there are some dark and light regions, it is not as obvious as for the 20 wt % addition levels in the aliphatic (R1) and slightly aromatic (R2) resin addition levels. It is interesting to note that at 30 wt % and 40 wt % addition levels of highly aromatic (14%) unsaturated resin (R3), containing OBC/PE–PP blend showed single tan δ peak, but the morphological analysis clearly shows ternary phase structures, which includes an OBC–resin continuous phase, light PE–PP–resin dispersed phase along with a resin dominated circular dark dispersed phase, as we seen for the OBC/PP blends containing highly aromatic (14%) unsaturated resin (R3). OBC/PP blends containing highly aromatic (14%) unsaturated resin (R3) DMA showed two tan δ peak which correlated well with the immiscibility characteristics observed in the morphological analysis. Even though we see a ternary phase morphology for OBC/PE–PP blends containing highly aromatic (14%) unsaturated resin (R3), the storage modulus, G' (Figure 15) of the blends, in between the parent polymers (lower than OBC and higher than PE–PP) indicates that the resin is in the OBC/PE–PP interphase, which improves the miscibility characteristics, resulting in a single tan δ peak. On the other hand, OBC/PP blends containing highly aromatic (14%) unsaturated resin (R3) showed lower modulus (G') than that of the parent polymers (Figure 10), indicating that the resin is softening both the parent polymer phases (especially OBC) more than that of the OBC/PP interphase, resulting in two tan δ peaks.

Since it has been observed that aromatic content or cyclic nature of the unsaturated hydrocarbon resin chemistry influences the compatibility behavior of the OBC/PP blends and OBC/PE–PP blends, it would be interesting to see the effect of saturated cycloaliphatic resins on the compatibility characteristics of OBC/PP and OBC/PE–PP blends. In the next section, the effect of a saturated cycloaliphatic hydrocarbon resin and a linear aliphatic–cycloaliphatic resin on OBC/PP blends and OBC/PE–PP blends will be discussed.

Effect of Saturated Hydrocarbon Resins on OBC/APO Blends

Viscoelastic properties measured using dynamic mechanical analysis (DMA) of the OBC/PP blends and OBC/PE–PP blends with two different saturated hydrocarbon resins are discussed first, followed by description of the morphological evaluation (TEM) of the OBC/PP and OBC/PE–PP blends. Dynamic mechanical analysis of the OBC/PP blends with cycloaliphatic resin (Resin 4) at three different concentrations is shown in Figure 20.

It can be seen from the above viscoelastic properties that both 20 and 30 wt % additions of cycloaliphatic saturated resin (R4) still show two glass transitions indicating immiscibility.

Applied Polymer SCIENCE

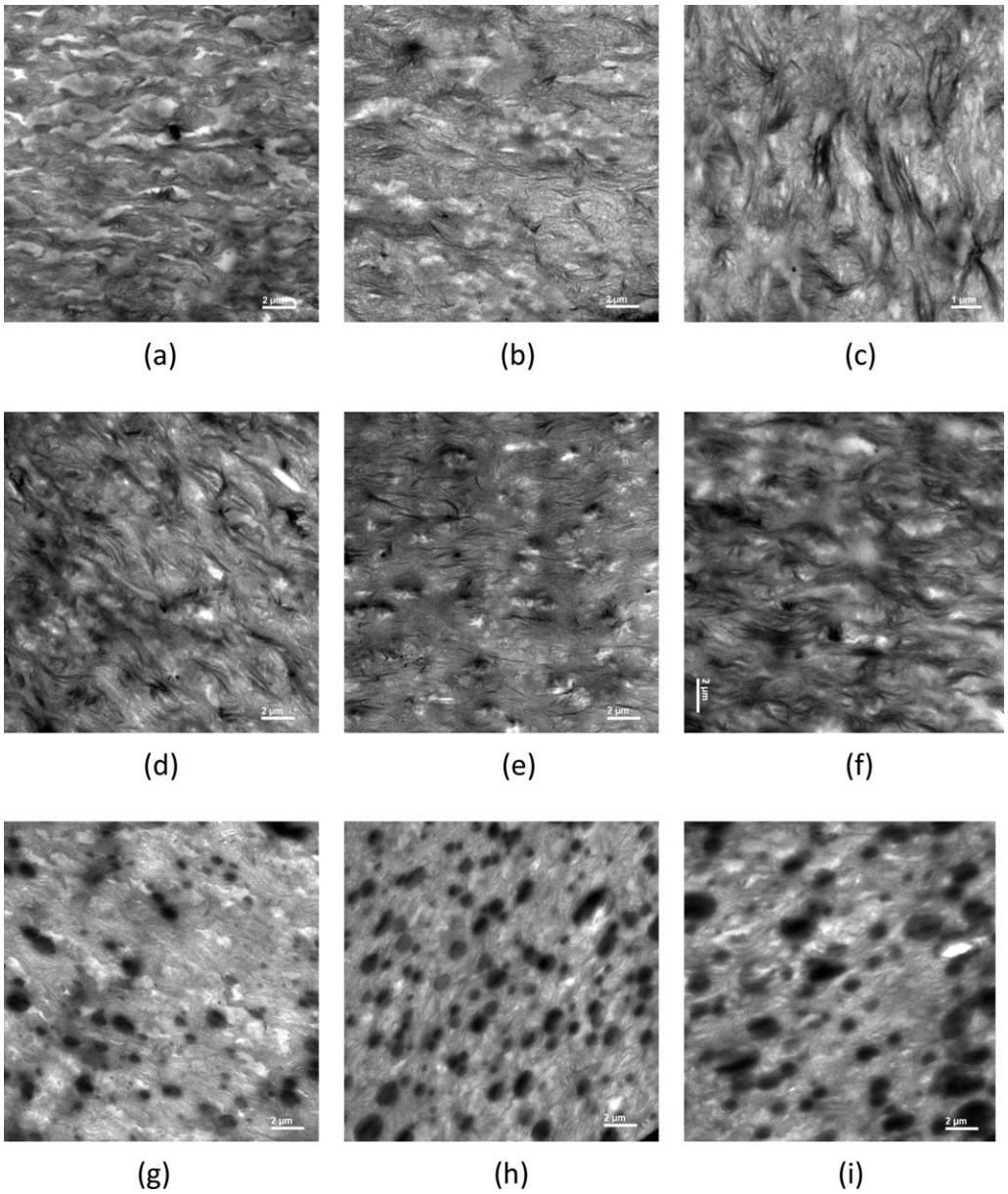

Figure 18. TEM micrographs of OBC/PP blend containing unsaturated resins. (a) 40/40/20 (OBC/PP/R1), (b) 35/35/30 (OBC/PP/R1), (c) 30/30/40 (OBC/PP/R1), (d) 40/40/20 (OBC/PP/R2), (e) 35/35/30 (OBC/PP/R2), (f) 30/30/40 (OBC/PP/R2), (g) 40/40/20 (OBC/PP/R3), (h) 35/35/30 (OBC/PP/R3), and (i) 30/30/40 (OBC/PP/R3).

However 40 wt % addition of cycloaliphatic saturated resin shows a single, broad glass transition. It should be noted that the first glass transition temperature and the second glass transition temperature significantly increased for the blends containing 20 and 30 wt % cycloaliphatic saturated resin (R4) indicating some degree of miscibility, and the decrease in G' shows softening of the respective polymers by the resin addition. The glass transition temperature for the 40 wt % aliphatic saturated resin containing blend is close to that of PP polymer and shows a broad tan δ peak. Elastic modulus (G') decreases as the amount of saturated cycloaliphatic resin in the blend increases and is lower than that of the parent polymers. This may be an indication of the softening of the individual polymers. Figure 21 shows the viscoelastic characteristics of OBC/PP blend containing linear aliphatic–cycloaliphatic saturated resin (R5) at different concentrations.

This follows the same trend as it has seen for the aliphatic saturated resin containing blends in previous work. Interestingly, blends containing 30 and 40 wt % of linear aliphatic–cycloaliphatic resin show a single, broad glass transition temperature, but the modulus is lower than that of the parent polymers.

Figure 22 shows the effect of cycloaliphaticity at 40 wt % addition levels for the saturated resin containing OBC/PP blends. In Figure 22, blends with cycloaliphatic and linear aliphatic–cycloaliphatic resin at 40 wt % addition level show

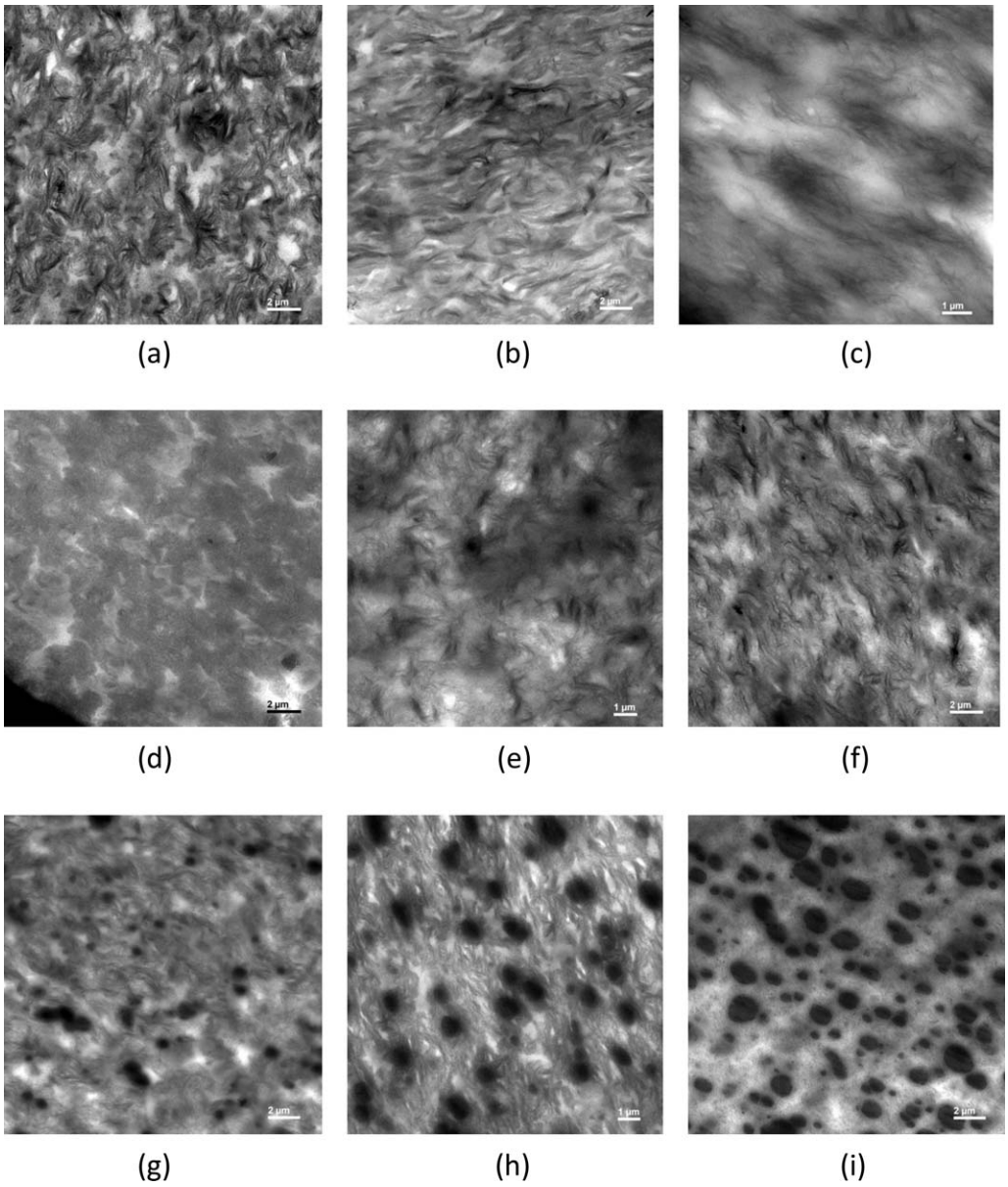

Figure 19. TEM micrographs of OBC/PE–PP blend containing unsaturated resins. (a) 40/40/20 (OBC/PE–PP/R1), (b) 35/35/30 (OBC/PE–PP/R1), (c) 30/30/40 (OBC/PE–PP/R1), (d) 40/40/20 (OBC/PE–PP/R2), (e) 35/35/30 (OBC/PE–PP/R2), (f) 30/30/40 (OBC/PE–PP/R2), (g) 40/40/20 (OBC/PE–PP/R3), (h) 35/35/30 (OBC/PE–PP/R3), and (i) 30/30/40 (OBC/PE–PP/R3).

similar viscoelastic behavior (single T_g, single narrow tan δ curve, and similar elastic modulus). There is not much difference in miscibility characteristics between the two resins in OBC/PP blends.

Interestingly Resin 5 shows slightly higher T_g for OBC/PP blends compared to blends containing cycloaliphatic saturated resin (R4), and this is mainly due to the higher softening point of Resin 5. Figure 23 shows the ternary plot of OBC/PP blends with saturated hydrocarbon resins, binary blends of OBC with saturated hydrocarbon resins and binary blends of PP with saturated hydrocarbon resins. In Figure 23, binary blends of OBC polymer with both saturated tackifier resins shows single T_g, and the cycloaliphaticity of resin has little effect on the compatibility. However, binary blends of PP with saturated hydrocarbon resins show a completely different behavior such that as the cycloaliphaticity in the resin increases, the compatibility also increases., resulting in a single T_g at all concentration levels of resin addition for the PP-R4 blends, as indicated by the clear dots. Figure 24 below shows the effect of aliphatic saturated resin in OBC/PE–PP blends at three different ratios.

From Figure 24, 30 and 40 wt % addition of cycloaliphatic saturated resin in to OBC/PE–PP blends show single glass

Applied Polymer SCIENCE

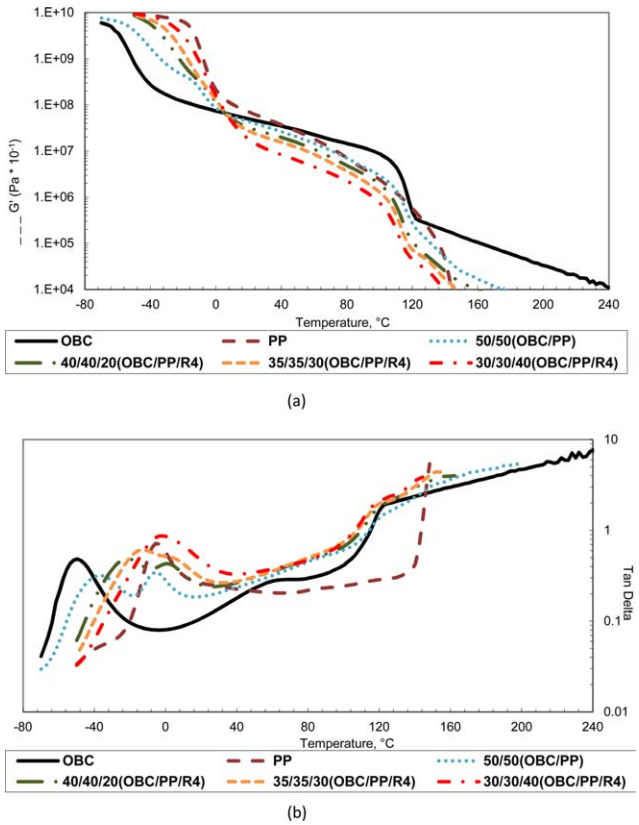

Figure 20. DMA of OBC/PP/cycloaliphatic saturated hydrocarbon resin blends at different ratios: (a) storage modulus and (b) Tan δ. [Color figure can be viewed in the online issue, which is available at wileyonlinelibrary.com.]

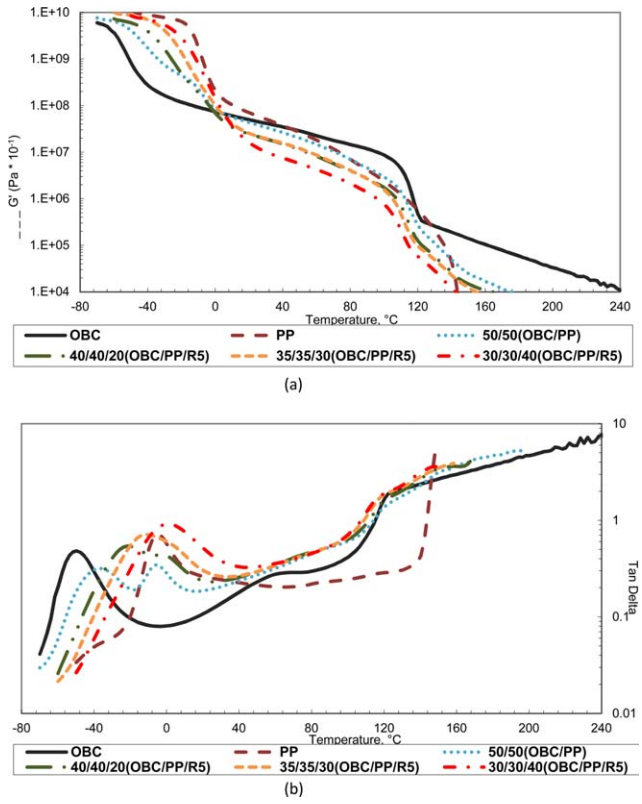

Figure 21. DMA of linear aliphatic–cycloaliphatic saturated hydrocarbon resin containing OBC/PP blends at different ratios: (a) storage modulus and (b) Tan δ. [Color figure can be viewed in the online issue, which is available at wileyonlinelibrary.com.]

transition and higher glass transition temperatures than that of the parent polymers. It is interesting to note that the storage modulus (G', at room temperature) of the blends containing 20, 30, and 40 wt % aliphatic saturated resin show similar trends. The storage modulus for these blends is intermediate between the individual polymer values without resin and lower than the 50/50 OBC/PE–PP polymer blend without any resin. This behavior is different than that of the OBC/PP blends containing cycloaliphatic saturated resins (Figure 20), in which the blends containing resins showed lower modulus than that of the parent polymers.

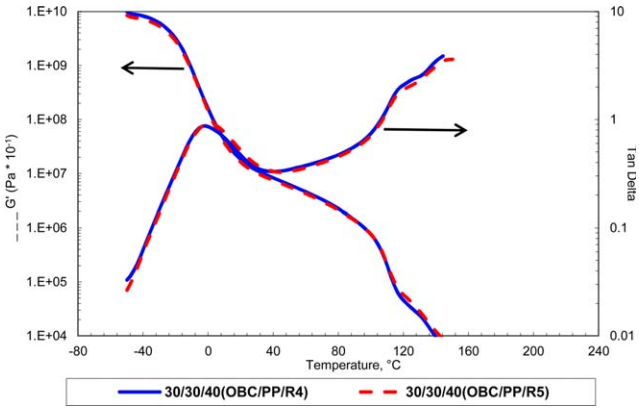

Figure 22. DMA of OBC/PP blends containing 40 wt % saturated hydrocarbon resin. [Color figure can be viewed in the online issue, which is available at wileyonlinelibrary.com.]

Figure 25 shows the viscoelastic properties of linear aliphatic–cycloaliphatic saturated resin containing OBC/PE–PP blend at different resin concentrations. Interestingly linear aliphatic–cycloaliphatic modified saturated resins improve the miscibility characteristics of the OBC/PE–PP blends, even at low resin addition amount (20 wt %) as can be seen in Figure 25. As the resin amount increases, the miscibility characteristic also improves resulting in single glass transition at 30 and 40 wt % resin addition. The elastic modulus also decreases as the resin concentration increases and the resulting storage modulus lies between both parent polymers and the 50/50 OBC/PE–PP blends.

As mentioned earlier, lower cycloaliphaticity (R5) of the resin actually has a definite influence in miscibility characteristics of OBC/PE–PP blends. OBC/PE-PP blends that contain 30 and 40 wt % resin addition amounts of linear aliphatic–cycloaliphatic resin shows a single T_g, a narrower tan δ curve and a lower elastic modulus, indicating improved miscibility. PE–PP polymer seems to improve the interfacial miscibility characteristics of OBC/PE–PP blend, when formulated with a saturated resin. Figure 26 shows the influence of saturated resin aromatic content on OBC/PE–PP blend.

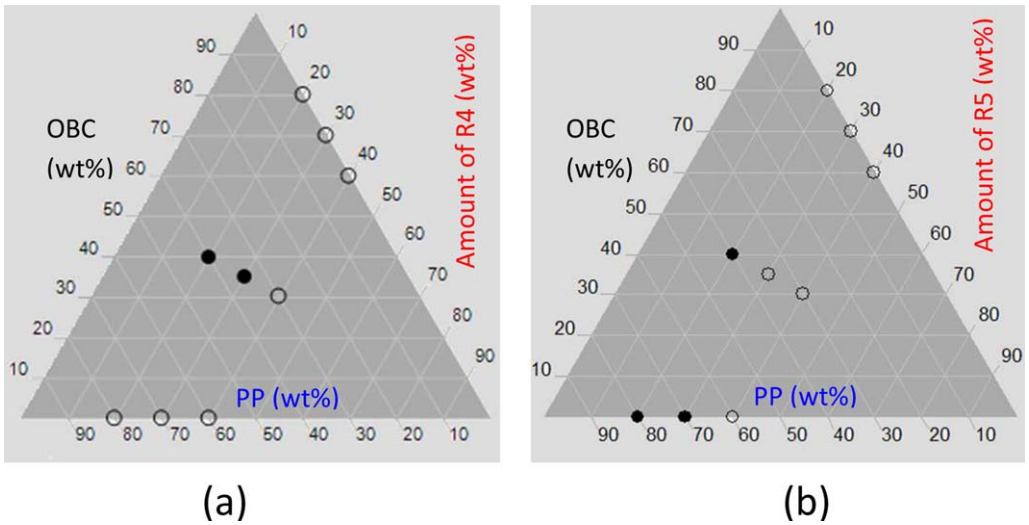

Figure 23. Ternary plot of glass transition temperatures for OBC/PP blends with resins. (a) Resin 4 (R4) and (b) Resin 5 (R5). [Color figure can be viewed in the online issue, which is available at wileyonlinelibrary.com.]

In Figure 26, the viscoelastic behavior of OBC/PE–PP blends with saturated hydrocarbon resins are very similar, indicating less influence on the resin chemistry (aliphatic and cycloaliphatic) at 40 wt % resin addition levels. Figure 27 shows the ternary plot of OBC/PE–PP blends with saturated hydrocarbon resins, binary blends of OBC with saturated hydrocarbon resins and binary blends of PE–PP with saturated hydrocarbon resins. In Figure 27, binary blends of OBC polymer with all three

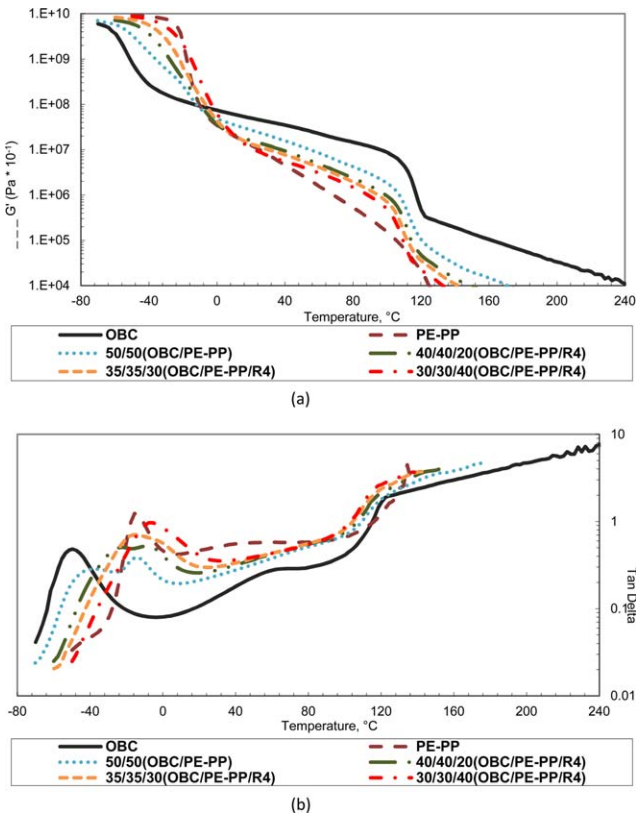

Figure 24. DMA of OBC/PE–PP/cycloaliphatic saturated hydrocarbon resin blends at different ratios: (a) storage modulus and (b) Tan δ. [Color figure can be viewed in the online issue, which is available at wileyonlinelibrary.com.]

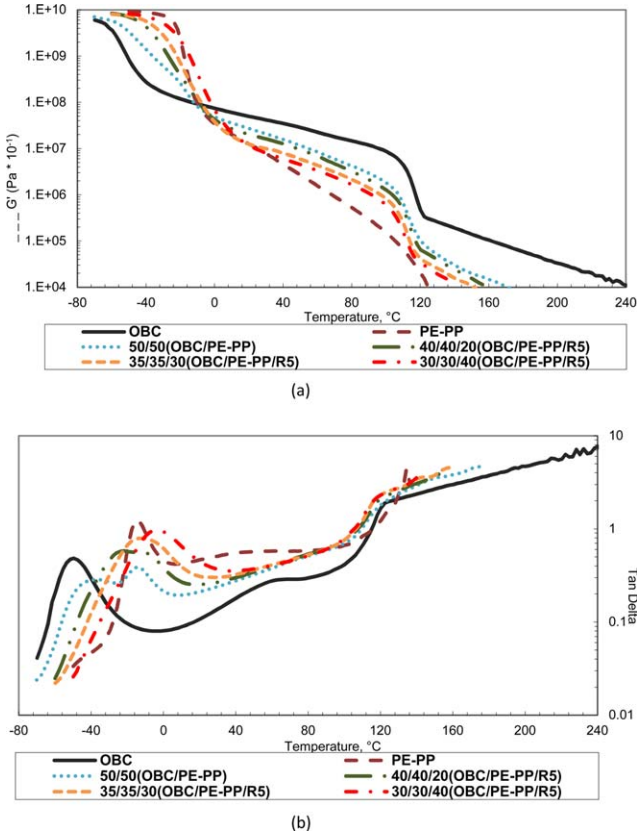

Figure 25. DMA of linear aliphatic–cycloaliphatic saturated hydrocarbon resin containing OBC/PE–PP blends at different ratios: (a) storage modulus and (b) Tan δ. [Color figure can be viewed in the online issue, which is available at wileyonlinelibrary.com.]

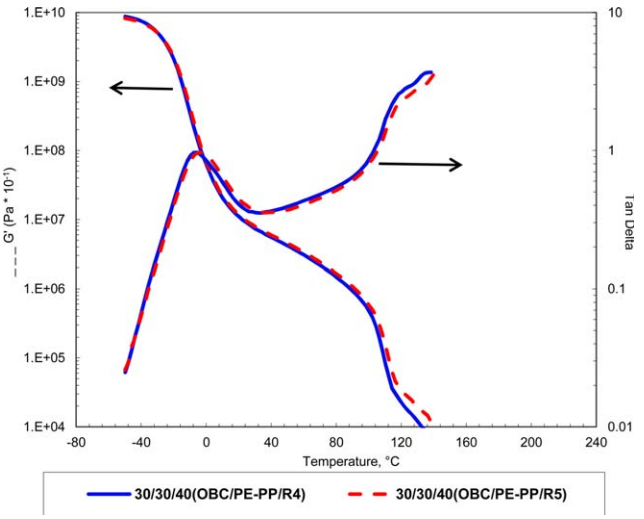

Figure 26. DMA of 40 wt % saturated resin containing OBC/PE–PP blends. [Color figure can be viewed in the online issue, which is available at wileyonlinelibrary.com.]

saturated tackifier resins shows single T_g, and the cycloaliphaticity of resin has little effect on the compatibility characteristics. Interestingly, binary blends of PE–PP with linear aliphatic–cycloaliphatic saturated hydrocarbon resins also show a single T_g, which is a completely different behavior than that of the PP–resin blends, which showed two T_g's at higher polymer concentration levels in the blends. The presence of propylene in the copolymer creates a more rigid backbone with a bulky methyl group, compared to more flexible linear polyethylene backbone. This could be the reason for the differences observed in the miscibility of the blends. Figure 28 shows the TEM micrographs of OBC/PP blends containing three different saturated resin levels.

The continuous phase and dispersed phase morphologies of the OBC/PP containing saturated resin blends are clear from the above TEM micrographs (Figure 28). TEM micrographs in rows show the morphology of blends containing the same saturated resin at different levels in the blend. The TEM micrographs in columns show the change of morphology created with different resin structures. The dark areas are the OBC polymer phase containing resin, and the light areas are dispersed phase of the PP APO with resin. Since it was difficult to selectively stain one of the phases due to the chemical nature of the blend components, the phase contrast is due to the density differences. The improved miscibility of the 40 wt % aliphatic saturated resins containing OBC/PP blend can be correlated well to the single T_g observed from DMA (Figures 20 and 21), compared to 20 wt % addition levels. Both resins (R4 and R5) being aliphatic in nature, it was very difficult to see any significant morphological differences between the blends through TEM. Phase morphologies of OBC/PE–PP blends with saturated resins (Figure 29) are similar to that of OBC/PP blends with saturated resins, in which the OBC–resin matrix forms the continuous phase while the PE–PP–resin matrix forms the dispersed phase. The continuous and dispersed phase morphologies of the blends containing cycloaliphatic saturated resin (R4) containing blends and linear aliphatic–cycloaliphatic resin (R5) containing OBC/PE–PP blend is not that obvious as in the previous OBC–PP blends. It has been learned that at lower resin addition levels (20 wt %) both blends (OBC/PP and OBC/PE–PP) are immiscible irrespective of the resin chemistry, while at higher resin addition levels (30 and 40 wt %) OBC/PP and OBC/PE–PP blends showed a single T_g, indicating improved miscibility with both resin chemistries. Continuous and dispersed phase morphologies were observed for both ternary blends using both resin chemistries.

Harkins spreading coefficient concept was used to better understand the ternary blend dispersed phase morphology. Mostofi et al.[32] and Hobbs et al.[33] reported a theoretical method to determine the phase morphology of ternary blend systems, especially the dispersed phase morphology. Both of the

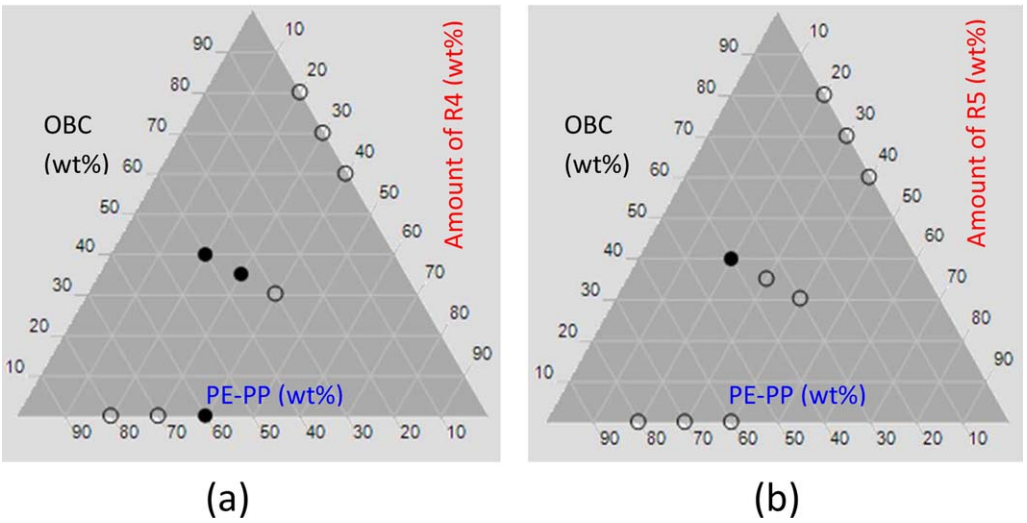

Figure 27. Ternary plot of glass transition temperatures for OBC/PE–PP blends with resins. (a) Resin 4 (R4) and (b) Resin 5 (R5). [Color figure can be viewed in the online issue, which is available at wileyonlinelibrary.com.]

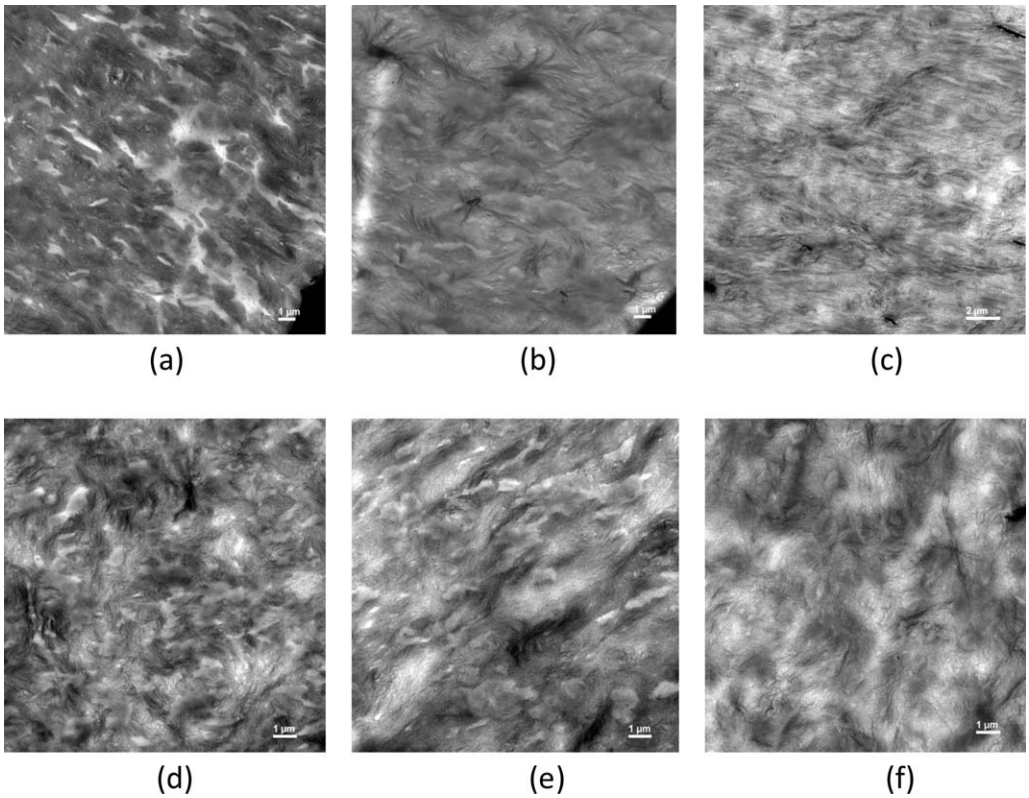

Figure 28. TEM micrographs of OBC/PP blend containing saturated resins. (a) 40/40/20 (OBC/PP/R4), (b) 35/35/30 (OBC/PP/R4), (c) 30/30/40 (OBC/PP/R4), (d) 40/40/20 (OBC/PP/R5), (e) 35/35/30 (OBC/PP/R5), and (f) 30/30/40 (OBC/PP/R5).

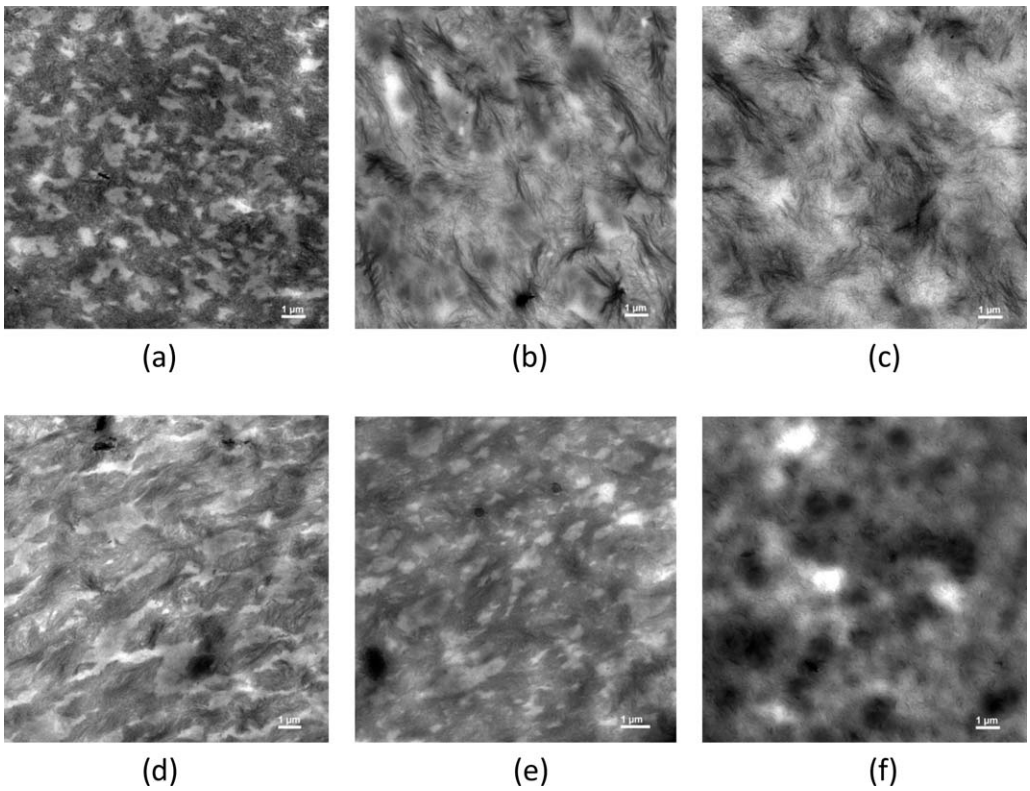

Figure 29. TEM micrographs of OBC/PE–PP blend containing saturated resins. (a) 40/40/20 (OBC/PE–PP/R4), (b) 35/35/30 (OBC/PE–PP/R4), (c) 30/30/40 (OBC/PE–PP/R4), (d) 40/40/20 (OBC/PE–PP/R5), (e) 35/35/30 (OBC/PE–PP/R5), and (f) 30/30/40 (OBC/PE–PP/R5)

Table VI. Surface Tension of OBC, PP, PE–PP, and Hydrocarbon Resins

	Surface tension (mN/m)		
Name	Dispersive portion (mN/m)	Polar portion (mN/m)	Total surface tension (mN/m)
Resin 1 (R1)	46.9	0.02	46.92
Resin 2 (R2)	48.04	0.03	48.07
Resin 3 (R3)	49.84	0.59	50.43
Resin 4 (R4)	50.33	0.13	50.46
Resin 5 (R5)	38.96	0.02	38.98
OBC	18.36	0.11	18.47
PP	24.66	0.27	24.92
PE–PP	23.55	0.6	24.15

researchers used Harkins spreading coefficient concept, specifically used for ternary blends containing a continuous phase A and dispersed phases B and C.[32] The spreading coefficients λ_{BC} and λ_{CB} are defined as follows:

$$\lambda_{BC}=\gamma_{AC}-\gamma_{AB}-\gamma_{BC} \quad \& \quad \lambda_{CB}=\gamma_{AB}-\gamma_{AC}-\gamma_{BC} \tag{1}$$

where "γ_{ij}" is the interfacial tension between components "i" and "j" phases and is defined as follows:

$$\gamma_{ij}=\gamma_i+\gamma_j-\frac{4\gamma_i^d\gamma_j^d}{\gamma_i^d+\gamma_j^d}-\frac{4\gamma_i^p\gamma_j^p}{\gamma_i^p+\gamma_j^p} \tag{2}$$

where γ_i and γ_j are the surface tension of the components 'i' and 'j'. γ_i^d and γ_j^d are the dispersive portions, and γ_i^p and γ_j^p are the polar portions of the surface tension component "i" and "j," respectively. Negative spreading coefficient values, "λ_{BC}" and "λ_{CB}" will result in separate dispersed phases of minor components. If spreading coefficient "λ_{BC}" is positive and spreading coefficient "λ_{CB}" is negative, it will result in encapsulation of "C" phase by "B" phase.[32]

Table VI shows the surface tension data obtained through contact angle measurements. Total surface tension is the sum of dispersive and polar portions. As the aromatic content of the hydrocarbon resins increases, the total surface tension also increases. Aliphatic–aromatic resin with high aromatic (14%) content show higher surface tension, not only in the dispersive portion, but also for the polar portion.

Polar portion of the surface tension for high aromatic content resin (R3) and PE–PP polymer are the same, while there is a significant difference in dispersive portions of the surface tension between the two. Cycloaliphatic resins show higher surface tension, not only in the dispersive portion, but also for the polar portion. The polar portion of the surface tension for cycloaliphatic resin (R4) and OBC polymer are the same, while there is a significant difference in dispersive portions of the surface tension between the two. There is not much difference between the total surface tension of the PP and PE–PP polymers, but both of them are higher than that of the OBC polymer.

The spreading coefficients calculated for OBC/PP/unsaturated hydrocarbon resin blends and OBC/PE–PP/unsaturated hydrocarbon resin blends are given in Table VII. As we seen from the blend morphologies, OBC is considered as the continuous phase "A". PP polymer and PE–PP polymer were considered as the dispersed phase "B". Resins R1, R2, R3, R4, and R5 were considered as the dispersed phase "C" for calculations.

As can be seen from Table VII that spreading coefficient "λ_{BC}" is positive and spreading coefficient "λ_{CB}" is negative, which will result in encapsulation of phase "C" by phase "B". This means that in case of all the blends, the hydrocarbon resin is encapsulated by the amorphous PP or amorphous PE–PP polymer in the dispersed phase, which depends on the blend composition.

Table VII. Spreading Coefficients Calculated for the OBC/PP/Resin and OBC/PE–PP/Resin Blends

Resin type	OBC/PP	OBC/PE–PP
Resin 1 (R1)	λ_{BC} = 4.45	λ_{BC} = 3.28
	λ_{CB} = −18.68	λ_{CB} = −19.84
Resin 2 (R2)	λ_{BC} = 4.63	λ_{BC} = 3.44
	λ_{CB} = −20.03	λ_{CB} = −21.22
Resin 3 (R3)	λ_{BC} = 5.26	λ_{BC} = 4.46
	λ_{CB} = −22.50	λ_{CB} = −23.30
Resin 4 (R4)	λ_{BC} = 5.08	λ_{BC} = 3.89
	λ_{CB} = −22.73	λ_{CB} = −23.91
Resin 5 (R5)	λ_{BC} = 3.07	λ_{BC} = 2.14
	λ_{CB} = −9.91	λ_{CB} = −10.83

CONCLUSIONS

- Unsaturated aliphatic hydrocarbon resins seem to show better compatibility characteristics with OBC/PP blends. However, aromatically modified aliphatic unsaturated hydrocarbon resins show better compatibility characteristics with OBC/PE–PP blends. Overall it has been observed that OBC/PE–PP showed better miscibility characteristics with unsaturated hydrocarbon resins than that of the OBC/PP blends with unsaturated hydrocarbon resins.

- Ternary blends of OBC/PP with unsaturated aliphatic resins at higher resin addition levels showed compatibility behavior. Higher the aromatic content of the resin (especially R3) in OBC/PP blend, lower the compatibility.
- A ternary phase morphology was particularly observed for both OBC/PP and OBC/PE–PP blends with highly aromatic (14%) hydrocarbon resin, in which OBC forming the continuous phase, and PP, PE–PP, and unsaturated hydrocarbon resins forming the dispersed phase with respective blend composition.
- Ternary blends of OBC/PE–PP with unsaturated hydrocarbon resins showed a completely different behavior than the OBC/PP/resin ternary blends. Higher the aromatic content of the unsaturated hydrocarbon resin for OBC/PE–PP blends, higher the compatibility. This is mainly due to the better interfacial interaction between the OBC/PE–PP interphase provided by the aromatically modified unsaturated resin chemistry. This is further verified though the storage modulus, G' (Figure 16) of the blends, in between the parent polymers for OBC/PP/R3 blends (lower than OBC and higher than PE–PP), which indicates that the resin is in the OBC/PE–PP interphase that improves the miscibility, resulting in compatibility (single tan δ peak). On the other hand OBC/PP blends containing highly aromatic (14%) unsaturated resin (R3) showed lower modulus (G') than that of the parent polymers (Figure 11), indicating that the resin is softening both the parent polymer phases (especially OBC) more than that of the OBC/PP interphase, resulting in incompatibility (two tan δ peak). However, the improved compatibility between PE–PP and OBC using aromatic hydrocarbon resin could also be from the resin pushing PE–PP toward the OBC/PE–PP interface, since these resins went into the PE–PP phase. Due to their high surface energy, the lower surface energy PE–PP would be pushed toward the low surface energy of OBC.
- It has been learned that OBC–PP and OBC/PE–PP blends showed better miscibility characteristics with both saturated aliphatic hydrocarbon resins, irrespective of the difference in resin chemistries. Resin chemistry did not impact miscibility of the blend in either blend system (OBC/PP and OBC/PE–PP) at the higher resin addition levels.
- Harkins spreading coefficient concept was used to better understand the ternary blend dispersed phase morphology and learned that chemistry of tackifier resins does not seem to influence the spreading coefficients.

Since OBC/PE–PP blends showed slightly better miscibility characteristics with unsaturated hydrocarbon resin chemistry and saturated hydrocarbon resin chemistry, we recommend evaluating this blend in a higher resin containing high T_g pressure-sensitive adhesive formulation, possibly used for disposable diaper construction adhesive applications, due to the similarity in viscoelastic characteristics between the blends and the typical disposable diaper construction adhesive.

ACKNOWLEDGMENTS

Authors thank Pete Dunckley of Eastman Chemical Company for his valuable advice, suggestions and support throughout the work. Authors thank Deborah Moroney, Chris Jones, Arved Harding and Yuqing Zhu of Eastman Chemical Company for their support in obtaining some of the data and analysis.

REFERENCES

1. Carothers, W. H.; Hill, J. W.; Kirby, J. E.; Jacobson, R. A. *J. Am. Chem. Soc.* **1930**, *52*, 5279.
2. White, J. L.; Choi, D. In Polyolefins: Processing, Structure Development and Properties; Hanser Gardner Publications Inc.: Cincinnati, **2005**.
3. Ziegler, K. W.; Gellert, H. G. US Pat. No. 2,699,457, **1955**.
4. Natta, G.; Pino, P.; Corradini, P.; Danusso, F.; Mantica, E.; Mazzanti, G.; Moraglio, G. *J. Am. Chem. Soc.* **1955**, *77*, 1708.
5. Elaston, C. T. US Pat. 3,645,992, **1970**.
6. Kaminsky, W.; Kulper, K.; Brintzinger, H. H.; Wild, F. R. W. P. *Angew. Chem. Int. Ed. Eng.* **1985**, *24*, 507.
7. Ewen, J.; Jones, R. L.; Razavi, A.; Ferrara, J. D. *J. Am. Chem. Soc.* **1988**, *110*, 6255.
8. Lai, S. Y.; Wilson, J. R.; Knight, G. W.; Stevens, J. C.; Chum, S. P. US Pat. 5,272,236, **1993**.
9. Stevens, J. C. *Stud. Surf. Sci. Catal.* **1994**, *89*, 277.
10. Minick, J.; Moet, A.; Hiltner, A.; Baer, E.; Chum, S. P. *J. Appl. Polym. Sci.* **1995**, *58*, 1371.
11. Arriola, D. J.; Carnahan, E. M.; Hustad, P. D.; Kuhlman, R. L.; Wenzel, T. T. *Science* **2006**, *312*, 714.
12. Wang, H. P.; Khariwala, D. U.; Cheung, W.; Chum, S. P.; Hiltner, A.; Baer, E. *Macromolecules* **2007**, *40*, 2852.
13. Khariwala, D. U.; Taha, A.; Chum, S. P.; Hiltner, A.; Baer, E. *Polymer* **2008**, *49*, 1365.
14. Li Pi Shan, C.; Yalvac, S.; Diehl, C.; Marchand, G.; Rickey, C.; Karjala, T.; Carvagno, T.; Dunckley, P. M.; Germinario, L. *30th International PSTC Technical Seminar, Orlando, FL*, **2007**.
15. Vasile, C. In Handbook of Polyolefins, 2nd ed.; Marcel Dekker Inc.: New York, **2000**.
16. Utracki, L. A. In Polymer Alloys and Blends; Hanser Gardner Publications Inc.: Cincinnati, **1989**.
17. Coleman, M. M.; Graf, J. F.; Painter, P. C. In Specific Interactions and the Miscibility of Polymer Blends; Technomic Publishing Company Inc.: Lancaster, **1991**.
18. Datta, S.; Lohse, D. J. In Polymeric Compatibilizers; Hanser Gardner Publications Inc.: Cincinnati, **1996**.
19. Koning, C.; Duin, M. V.; Pagnoulle, C.; Jerome, R. *Prog. Polym. Sci.* **1998**, *23*, 707.
20. Kulshreshtha, A. K.; Vasile, A. K. In Handbook of Polymer Blends and Composites; Rapra Technology Limited: Shawbury, UK, **2003**.
21. Krause, S. *Pure Appl. Chem.*, **1986**, *58*, 1553.
22. Sheout, W. H.; Day, H. H. US Pat. 3965, **1845**.
23. Drew, R. G. GB Pat. 3,12,610, **1930**.
24. Drew, R. G. GB Pat. 4,05,263, **1934**.
25. Class, J. B.; Chu, S. G. *J. Appl. Polym. Sci.* **1985**, *30*, 805.

26. Satas, D. In Handbook of Pressure Sensitive Adhesive Technology, *3rd ed.*; Satas & Associates: Warwick-RI, **1999**.
27. Nakajima, N.; Babrowicz, R.; Harrell, E. R. *J. Appl. Polym. Sci.* **1992**, *44*, 1437.
28. Dunckley, P. M. *Adhes. Age*, November **1993**, 17.
29. Yau, S. N.; Woo, E. M. *Macromol. Rapid Commun.* **1996**, *17*, 615.
30. Hamdan, S.; Hashim, D. M. A.; Ahmad, M.; Embong, S. *J. Polym. Res.*, **2000**, *7*, 237.
31. Robeson, L. M. In Polymer Blends; Hanser Gardner Publications Inc.: Cincinnati, **2007**.
32. Mostofi, N.; Nazockdast, H.; Mohammadigoushki, H. *J. Appl. Polym. Sci.* **2009**, *114*, 3737.
33. Hobbs, S. Y.; Dekkers, M. E. J.; Watkins, V. H. *Polymer*, **1988**, *29*, 1598.